NeuroImage: Clinical 11 (2016) 210–223

Contents lists available at ScienceDirect

NeuroImage: Clinical

journal homepage: www.elsevier.com/locate/ynicl

Alpha desynchronization and fronto-parietal connectivity during spatial working memory encoding deficits in ADHD: A simultaneous EEG-fMRI study

Agatha Lenartowicz[a,b,*], Steven Lu[a], Cameron Rodriguez[a], Edward P. Lau[a], Patricia D. Walshaw[a,b], James T. McCracken[a,b], Mark S. Cohen[a,b,c], Sandra K. Loo[a,b]

[a]Semel Institute for Neuroscience and Human Behavior, 760 Westwood Plaza, Los Angeles, CA 90024, United States
[b]David Geffen School of Medicine, 760 Westwood Plaza, Los Angeles, CA 90024, United States
[c]California Nanosystems Institute, 760 Westwood Plaza, Los Angeles, CA 90024, United States

ARTICLE INFO

Article history:
Received 15 December 2015
Received in revised form 23 January 2016
Accepted 31 January 2016
Available online 6 February 2016

Keywords:
Alpha
Functional connectivity
Spatial working memory
Encoding
ADHD
EEG-fMRI

ABSTRACT

The underlying mechanisms of alpha band (8–12 Hz) neural oscillations are of importance to the functioning of attention control systems as well as to neuropsychiatric conditions that are characterized by deficits of that system, such as attention deficit hyperactivity disorder (ADHD). The objectives of the present study were to test if visual encoding-related alpha event-related desynchronization (ERD) correlates with fronto-parieto-occipital connectivity, and whether this is disrupted in ADHD during spatial working memory (SWM) performance. We acquired EEG concurrently with fMRI in thirty boys (12–16 yrs. old, 15 with ADHD), during SWM encoding. Psychophysiological connectivity analyses indicated that alpha ERD during SWM encoding was associated with *both* occipital activation and fronto-parieto-occipital functional connectivity, a finding that expands on prior associations between alpha ERD and occipital activation. This finding provides novel support for the interpretation of alpha ERD (and the associated changes in occipital activation) as a phenomenon that involves, and perhaps arises as a result of, top-down network interactions. Alpha ERD was associated less strongly with occipital activity, but associated more strongly with fronto-parieto-occipital connectivity in ADHD, consistent with a compensatory attentional response. Additionally, we illustrate that degradation of EEG data quality by MRI-amplified motion artifacts is robust to existing cleaning algorithms and is significantly correlated with hyperactivity symptoms and the ADHD Combined Type diagnosis. We conclude that persistent motion-related MR artifacts in EEG data can increase variance and introduce bias in interpretation of group differences in populations characterized by hypermobility — a clear limitation of current-state EEG-fMRI methodology.

1. Introduction

Working memory (WM), the ability to store and manipulate information transiently in memory (Baddeley, 1986, 2002), is one of core functions affected in attention deficit hyperactivity disorder (ADHD) (Castellanos and Tannock, 2002; Nigg, 2005); it is also one of the most perplexing. In support of WM system dysfunction in ADHD, group differences in behavioral performance on WM tasks consistently show medium to large effect sizes (Alderson et al., 2013; Boonstra et al., 2005; Kofler et al., 2013; Loo et al., 2007; Martinussen et al., 2005; Westerberg et al., 2004; Willcutt et al., 2005), and neuroimaging evidence indicates that patients with ADHD differ in fronto-parietal, or so called "top-down", circuitry associated with WM (Arnsten and Rubia, 2012; Bush, 2010; Castellanos and Tannock, 2002; Rubia et al., 2014). Yet stimulant medications, which target such circuitry and offer relief from related symptoms such as sustained attention or response inhibition, are inconsistent in alleviating WM symptoms (Rubia et al., 2013; Rubia et al., 2014). Moreover, spatial orienting and effects of load in WM, both of which also rely on fronto-parietal network integrity, have demonstrated a lack of group differences (Bedard et al., 2014; Huang-Pollock and Nigg, 2003; Huang-Pollock et al., 2005; Wolf et al., 2009). Such findings prompt further study of the mechanism by which dysfunction of fronto-parietal circuitry contributes to SWM deficits in ADHD.

We have demonstrated recently (Lenartowicz et al., 2014) that within a spatial working memory (SWM) delayed match-to-sample task distinct group differences may be observed during different stages of the task: preparing for WM storage, encoding content into WM, and maintaining that content in WM. The most pronounced group differences in neural responses were present during the encoding phase of the task, before WM was engaged by the maintenance delay and before

* Corresponding author at: Semel Institute for Neuroscience and Human Behavior, 760 Westwood Plaza, Los Angeles, CA 90024, United States.
E-mail address: alenarto@g.ucla.edu (A. Lenartowicz).

http://dx.doi.org/10.1016/j.nicl.2016.01.023

items were to be retrieved from WM. We found that in children with ADHD event-related desynchronization (ERD) of alpha-frequency (8–12 Hz) neural oscillations during encoding was attenuated and predictive of ADHD symptoms and WM task performance. The involvement of alpha during encoding is notable, as it points to atypical fronto-parietal interactions with occipital cortex during the encoding process.

Alpha modulation during visual perception and attention has been hypothesized to be a functional mechanism by which information is selected or gated in visual cortex (Foxe and Snyder, 2011; Klimesch, 2012; Klimesch et al., 2011; Mathewson et al., 2011). Alpha ERD magnitude varies with task variables such as degree of semantic content (Klimesch, 1997; Klimesch et al., 2011), memory load and retrieval accuracy (Jensen et al., 2002; Klimesch, 1999; Klimesch et al., 1997), and visuospatial attention (Foxe and Snyder, 2011; Thut et al., 2006). Unlike other spectral phenomena (e.g., theta), ERD can reverse in sign (becoming an event-related synchronization, ERS) for stimulus inputs that are to be ignored (Foxe and Snyder, 2011; Rihs et al., 2007). Moreover, alpha ERD is thought to arise independent of perceptual processing (Klimesch et al., 2011), as it can occur before (Ergenoglu et al., 2004; Hanslmayr et al., 2007; Romei et al., 2010) or after (Freunberger et al., 2008) the stimulus, and can be absent during a stimulus when no post-perceptual processing is required (Hanslmayr et al., 2005).

Thus weakened alpha ERD in ADHD is a likely indicator of weakened top-down control during SWM encoding and, given prior association of fronto-parietal circuitry with both SWM (Awh and Jonides, 2001; Constantinidis et al., 2001; Smith and Jonides, 1997) and with alpha power (de Munck et al., 2007; Laufs et al., 2003; Liu et al., 2014; Scheeringa et al., 2009), it predicts weakened interactions between the fronto-parietal network and occipital cortex during encoding. In the context of ADHD, a confirmation of this hypothesis would imply that SWM deficits may hinge on relatively early attention control processes, and the success of these processes may directly influence the success of WM and, consequently, the presence or absence of group differences on WM tasks.

The objective of our study was therefore to test if encoding-related alpha ERD reflects fronto-parieto-occipital connectivity, whether this is disrupted in ADHD, and whether it predicts ADHD symptoms or SWM performance. While numerous studies have documented the relationship between alpha and activation in occipital, frontal and parietal cortices (de Munck et al., 2007; Goldman et al., 2002; Laufs et al., 2003; Liu et al., 2014; Moosmann et al., 2003; Scheeringa et al., 2009), the relationship between alpha and *connectivity* among these regions has not been established firmly. Multiple studies have reported fronto-parietal synchronization in the alpha range during WM tasks based on neurophysiological signals (Doesburg et al., 2009; Hummel and Gerloff, 2005; Palva and Palva, 2011; Sauseng et al., 2005; von Stein et al., 2000). However the experiment of combining EEG and fMRI in concurrent recordings to test directly if alpha modulation predicts inter-regional connectivity has been reported only by Scheeringa et al. (2012), who described decreased within-occipital connectivity during alpha ERS, but this manuscript did not include findings on alpha ERD. Moreover, a handful of studies have examined alpha related *activation* during SWM focusing on the maintenance interval and theta, using either concurrent EEG-fMRI (Michels et al., 2010; Michels et al., 2012; Scheeringa et al., 2009) or cross-subject EEG-fMRI correlations (Meltzer et al., 2007). Scheeringa et al. (2009) additionally examined alpha ERS during maintenance and reported an increase in frontal cortex, and a decrease in occipital cortex activity, which would be expected subsequent to encoding.

Finally, within ADHD, we are aware of four studies that have examined BOLD correlates of EEG signals, namely of event-related potential markers of reward (Boecker et al., 2014; Hauser et al., 2014), and of voluntary response selection (Karch et al., 2010; Karch et al., 2014), but not of encoding processes. It is notable that even within studies that employed EEG without fMRI we are aware of only two, other than our own, that have examined alpha ERD during encoding in WM (Gomarus et al., 2009; Missonnier et al., 2013). Thus whether alpha ERD reflects fronto-parieto-occipital functional connectivity, and if this relationship accounts for ADHD deficits in SWM, are both questions that warrant further study.

In the present experiment we used concurrent EEG-fMRI methodology to record both alpha ERD during encoding and associated changes in BOLD activity, and connectivity signals during SWM tasks in children with and without ADHD. The results confirm prior associations between alpha and occipital activation, expand this association to include fronto-parietal-connectivity, and demonstrate differences between children with and without ADHD in both relationships. Additionally, our findings suggest caution in EEG-fMRI assessment of populations characterized by hypermobility, such as children with ADHD Combined Type diagnosis, due to severe degradation of EEG data by MRI-amplified motion related artifacts.

2. Methods

2.1. Participants and diagnoses

A total of 30 boys (15 with ADHD, 12–16 years old) were recruited from the Los Angeles community through flyers, community organizations (CHADD; www.chadd.org), and the UCLA ADHD clinic. Exclusion criteria included: IQ < 80, history of learning disabilities, co-morbid Axis I diagnoses other than oppositional defiant disorder, and current use of psychotropic medications other than psychostimulants. Parents/participants received verbal and written explanations of study requirements and, prior to any study procedures, provided written informed permission/assent as approved by the UCLA Institutional Review Board. No participants, including those diagnosed with ADHD, were on medication during clinical assessment or testing, withholding use 24–48 h prior to session, consistent with medication half-life.

We evaluated children for ADHD and other psychiatric disorders through a semi-structured diagnostic interview with the primary caretaker (usually the mother) and a direct interview with the child using the Schedule for Affective Disorders and Schizophrenia for School-Age Children (KSADS-PL) (Kaufman et al., 1997). Psychiatric disorders were considered present if the participant currently met full DSM-IV diagnostic criteria for any ADHD subtype. Two clinical psychologist trainees conducted all interviews. Senior clinicians (SKL, PDW) confirmed psychiatric diagnoses after individual review of symptoms, developmental course, and impairment level. We assessed full scale intelligence (FSIQ) using the Wechsler Abbreviated Scale of Intelligence (WASI), learning disability using the reading comprehension and word reading scales of the Wide Range Achievement Test 4 (WRAT), and severity of ADHD symptoms using the Strengths and Weaknesses of ADHD symptoms and Normal (SWAN) Behavior Scale (Swanson et al., 2006). Positive scores on the SWAN scale indicate more symptoms, whereas negative scores indicate fewer symptoms.

2.2. Task

We used a computerized version of the spatial working memory (SWM) task (Glahn et al., 2002; Sternberg, 1966) to assess alpha ERD during WM encoding (Fig. 1), the timing of which was adapted for fMRI. Each trial consisted of a fixation cross for 500-msec, followed by an encoding display containing 3 or 5 yellow dots (load), presented on a black background. After 2 s, the screen turned blank and remained blank for a maintenance interval of 7, 8 or 9 s, selected randomly on each trial. Next a single dot (probe) was presented for 3 s in either a location previously shown (match) or not (non-match). Participants were instructed to indicate using a left/right button press if the probe was a match or non-match to the encoding stimulus. Trials were separated by an inter-stimulus-interval (7, 8, or 9 s duration, randomized) during which the screen was blank. Of primary interest in this study were alpha ERD and neural activity/connectivity during the encoding period. We

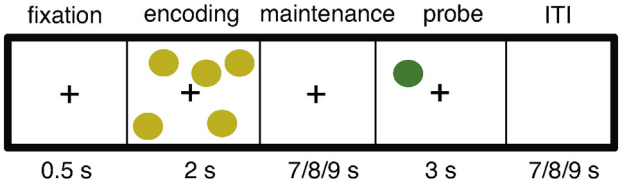

Fig. 1. Spatial working memory task. The appearance of an alerting fixation-cross cued trial onset. The encoding stimulus was either 1 or 5 dots. Following a 7, 8 or 9 s maintenance period, the probe stimulus appeared. Participants indicated, by button press, whether or not the location of the probe matched the location of any of the encoding stimulus dots. ITI: inter-trial interval.

also recorded accuracy, reaction time (RT) and standard deviation of reaction time (RTsd) as an index of response variability.

During the scanning session participants performed a total of 32 trials in each experimental block, and 2 blocks in total (12–13 min/block). In each block there were equal numbers of trials for each load and match/no-match response type. Encoding stimuli were also balanced in the spatial distribution of dots across upper/lower, and left/right visual field to ensure balanced but variable (across trials) visuospatial neural responses. Stimulus types were randomized across trials. Participants also performed a 2 min stimulus localizer task during which the same stimuli as used for the task were presented at brief succession (1 s duration, 250 ms inter-stimulus interval) in mini-blocks of 4 stimuli (~5 s/mini-block). The inter-block duration was 10 s, and a total of 8 blocks were presented. Participants were instructed to ignore the stimuli, to look at a central fixation cross, and to count how many times the fixation cross changed color to red (a total of 4 color changes were presented randomly). This condition was designed as a localizer to identify regions that respond to the visual stimuli without engaging visuo-spatio encoding mechanisms. It thus provided an unbiased prior on selecting seed regions that respond to the visual stimuli, and thus whose connectivity during SWM encoding may be related to alpha ERD, our central hypothesis.

Prior to scanning, children performed a 30 min practice session of the SWM task. They received an overview of the task, then performed 5 practice trials in which the response period was unlimited, allowing them to ask questions. This was repeated if desired. Children then performed one full block of the task (32 trials), in which the inter-trial interval was shortened to 3 s (Lenartowicz et al., 2014) to minimize fatigue. Following practice, we collected a 3 min recording during which participants alternated between 30 s intervals of sitting quietly with either eyes closes (EC) and eyes open (EO). This recording was used to establish a prior on the spatial distribution across electrodes of alpha modulation, which is expressed strongly with opening and closing of eyes (Berger, 1930; Kirschfeld, 2005).

All stimuli were generated using an Apple MacBook Pro Laptop Computer (Cupertino, CA). We controlled stimulus presentation and response collection using PsychToolbox Software (Brainard, 1997; Kleiner et al., 2007), running in Matlab (7.10 R2010a, Mathworks, Natick, MA). During scanning, stimuli were presented to participants by a projector and two-way mirror mounted on the MRI head coil, and participants responded using an MR-compatible button box, using their index and middle finger for left/right responses. During practice the stimuli were presented on a Dell Monitor, in a private testing room, and responses were collected using the left/right arrow keys of a QWERTY keyboard.

2.3. EEG-fMRI data collection

2.3.1. fMRI

The MRI data were acquired with a 3 T Siemens Trio MRI scanner (Erlangen, Germany). We collected T2*-weighted echoplanar images (EPI) [slice thickness, 3 mm; 36 slices; repetition time (TR), 2.16 s; echo time (TE), 30 ms; flip angle, 90°; matrix, 64 × 64; field of view (FOV), 192 mm] during each SWM task block and stimulus localizer. To facilitate registration of EPI images to Montreal Neurological Institute (MNI) space, we collected a T2-SPACE structural image [TR, 3.2 s; TE 213 ms; FOV, 256 mm; matrix, 256 × 256; sagittal plane; slice thickness, 1 mm; 224 slices], and T2-weighted matched bandwidth high-resolution structural scan with the same slice prescription as the EPIs.

2.3.2. EEG

The EEG data during each SWM block were acquired concurrently with the MR data using Electrical Geodesics (Eugene, OR) GES300 MR system, NetStation v4.54 recording software, sampling at 1000 Hz and clock synchronized to the MR EPI acquisition. We used 256-channel high-impedance HydroCel Geodesic Sensor Nets, with reference at vertex. Nets were positioned on each participant by aligning the vertex electrode with the vertex of the head, identified at the midpoint of the anion-to-inion and left/right preauricular landmarks. Electrode impedances were <50 kΩ, as recommended by the manufacturer. Two additional external electrocardiogram (ECG) electrodes were applied to the chest (positions: left midclavicular line in 5th intercostal space and 4th left intercostal space at sternal border) for later use in suppression of artifacts as described below.

2.4. Analysis

2.4.1. Demographics, symptoms & performance

We used independent sample t-tests to assess group differences in age, FSIQ, verbal proficiency (WRAT), and symptoms (SWAN). We analyzed task accuracy, reaction time (RT) and its standard deviation (RT_{sd}) (an index of response variability) using repeated-measures ANOVA. Each analysis included the between-subject factor of GROUP (ADHD vs. TD controls) to test for overall differences in performance by the two diagnostic groups, and the within-subject factor of LOAD (1 dot at low load vs. 5 dots at high load) to test if performance differs with increasing load on WM, as well as their interaction. Analyses were performed using SPSS (IBM Corporation, Somers, NY).

2.4.2. fMRI preprocessing

Data processing was carried out using FSL software (www.fmrib.ox.ac.uk/fsl, S. M. Smith et al., 2004). First, the brain was isolated from the surrounding tissue using BET. Then, to correct for subject motion, functional images in each block were realigned to the middle volume by applying a rigid body (6 degrees of freedom) transformation using a normalized correlation similarity function with trilinear interpolation. The motion parameters from each transformation were retained for subsequent analysis. Data were smoothed spatially using a 5 mm full-width-half-maximum Gaussian kernel, filtered temporally using a non-linear high-pass filter with a 100 s cut-off, and grand-mean intensity normalized. Additionally, the data were denoised by means of probabilistic independent components analysis (Beckmann and Smith, 2004). Artifact components were labeled using a hierarchical supervised classification framework (Salimi-Khorshidi et al., 2014) and then were subtracted from the data. To establish the efficacy of this two-step motion removal approach we re-ran the motion correction realignment algorithm on the ICA denoised data and compared the motion parameters across groups. Following cleaning none of the six motion parameters showed significant differences between ADHD and TD groups, $t(28) < 1$, $p > .33$. This is in contrast to pre-cleaning motion parameters that indicated greater translational motion in ADHD than in TD participants, $t(28) > 1.9$, $p < .05$, suggesting that our strategy was sufficient to remove gross motion-related differences between groups. Last, the functional images were registered to the matched-bandwidth high-resolution scan, then to the T2-SPACE structural image, and finally into standard (Montreal Neurological Institute [MNI]) space, using affine transformations.

2.4.3. fMRI localizer analysis

The stimulus localizer scan was used to identify regions of interest (ROIs) for subsequent analyses of connectivity and relationship with alpha ERD. Analysis was conducted using FSL by fitting a generalized linear model to the time-series for each voxel. The model contained five event and two nuisance regressors. Event regressors were constructed for each stimulus mini-block type (dot stimuli presented in each of four visual quadrants) as well as for the 4 target events. For each regressor, trials were dummy coded as 1 s, with duration determined by event/mini-block duration, and were then convolved with a double-gamma hemodynamic response function (Glover, 1999). Temporal derivatives of each event predictor also were included as regressors to increase model sensitivity. Inter-block intervals were not modeled, and constitute an implicit baseline. Nuisance regressors included timeseries for two ROIs constructed in ventricles and white matter to model global signal changes unrelated to gray matter activation. Motion-parameter regressors were omitted, based on a validation analysis in which we performed all analyses with and without motion-parameter regressors and determined that event-related contrast results were largely unchanged. This additionally confirmed that our combined motion-correction and ICA denoising procedure was effective in eliminating motion-related variance in the data, and inclusion of motion-parameter regressors would unnecessarily account for additional degrees of freedom in the model. Finally, the data were pre-whitened to correct for temporal autocorrelation (Woolrich et al., 2001) before the final model fit was estimated using FILM.

We identified activation maps corresponding to dot stimuli by comparing parameter magnitudes across event regressors within a multi-level linear modeling framework (Beckmann et al., 2003), including robust group analysis using outlier inference (Woolrich, 2008). Whole-brain analyses were performed at the group-level, using mixed-effects analysis, and by including contrasts for assessment of mean stimulus response across all participants, as well as for an effect of GROUP (ADHD vs. TD). Group level parameter maps were thresholded using cluster detection statistics, with a height threshold of $z > 2.3$ and cluster probability of $p < 0.05$, and corrected for whole-brain multiple comparisons using Gaussian random field theory (Worsley and Friston, 1995). Finally we selected ROIs, used subsequently in the *EEG-fMRI analyses*, by identifying the location of peak activations during stimulus presentation. These ROIs were right lateral occipital cortex (rOccLat, x = 20 mm, y = −94 mm, z = 2 mm), right superior occipital cortex (rOccS, x = 26 mm, y = −62 mm, z = 52 mm) and right frontal eye fields (rFEF, x = 32 mm, y = −4 mm, z = 46 mm). The mean stimulus activation also included a peak in left superior occipital cortex, homologous to rOccS, however, since the examined effects did not differ from those of rOccS, they are not reported.

2.4.4. EEG preprocessing

Offline EEG processing and analyses were performed using custom MATLAB (V.7.14, R2012A, The Mathworks, Inc.) scripts using functions from the EEGLAB environment (v.13.x (dev), Delorme and Makeig, 2004). The EEG data were high-pass filtered (>.1 Hz). For EEG data collected concurrently during fMRI, gradient-related artifacts generated during each TR of scanning were removed using a template subtraction approach whereby the mean artifact, time locked to the MRI scanner's internal clock (MS Cohen, "*Method and apparatus for reducing contamination of an electrical signal*." USPTO. *Assigned to* The Regents of the University of California (Oakland, CA, US), 10/344,776, 7,286,871. 10/23/2007) is subtracted from each TR. The timeseries were then downsampled to 250 Hz and trimmed to remove residual gradient artifact at the beginning and end of the timeseries. Next, we inspected all data for noisy electrodes, which were interpolated.

For EEG data collected concurrently with fMRI, we additionally removed ballistocardiogram effects (Debener et al., 2008; Mullinger et al., 2013). This was done in two steps. First we used a template-based approach (Allen et al., 1998) to identify and then subtract the mean BCG artifact from each BCG event. Our approach was adapted to identify the heartbeat events in the EEG data (i.e., BCG events) rather than in the EKG data (i.e., EKG events) as typically reported (Allen et al., 1998). This approach was adopted because: (a) we found EKG recordings in children to be variable and not always reliable, (b) we found the timing between EKG and BCG peak events to be variable across children and not consistent with published recommendations (Debener et al., 2008) and, thus, (c) the EEG-based approach allowed us to model the BCG directly from the data. We have found that the timing of the BCG relative to the ECG events within an individual is highly reliable and thus provides at least as good if not better estimate of the BCG artifact (Rodriguez et al., 2013). In the second step the BCG-template cleaned data were decomposed into maximally independent component (IC) processes by temporal ICA decomposition using extended infomax (Lee et al., 1999) (stopping weight = 1e−7, maximum learning steps = 1000). We identified ICs that captured residual BCG artifact by creating an event-related average for each IC, time-locked to BCG peaks, and then correlating the BCG event-related timeseries with the BCG template. Significantly correlated ICs were subtracted from the Data. ICA was performed also in EEG data collected outside of the scanner (during practice session), and in all data we inspected spectral, spatial and temporal properties of each IC to identify artifacts due to eye movement and high-frequency noise. These ICs were also subtracted from the data.

The cleaned data were re-referenced to average reference. Next we extracted epochs time-locked to the onset of the encoding stimulus, beginning 1.4 s before and ending 15.4 s after the 2 s stimulus presentation. This 16-s time interval encompassed the entire duration of the trial including encoding, maintenance and probe, for visualization and reference to our previously published results (Lenartowicz et al., 2014). Using these relatively long epochs also served to circumvent edge effects in the time/frequency decomposition. Epochs containing any remaining artifacts, or followed by incorrect responses, were removed. To calculate event-related spectral perturbations (ERSPs), we applied Morlet wavelet decomposition, as implemented in EEGLAB *newtimef*(), to the epoch component time series. To identify alpha ERD effects we calculated power for 100 log-spaced frequencies ranging from 3 Hz to 125 Hz, and along 450 linearly spaced time bins (advanced in 38-ms steps) across the epoch. To adjust for the trade-off between frequency and temporal resolution, the wavelets were modified such that 3 cycles were used at the lowest frequency (3 Hz), increasing linearly to 25 cycles at the highest frequency (125 Hz). For group analyses, these trial spectrograms were averaged, converted to dB units, and baseline corrected by subtracting the log-power of the baseline period (also in dB) preceding onset of the fixation cross (−1400 ms to −100 ms) at each frequency from the log spectrogram values at each latency.

Alpha ERD then was extracted by averaging the ERSP magnitude across all latencies of the encoding stimulus (0–2 s) and within 8–12 Hz frequency band, as well as across occipital electrodes. These electrodes were selected based on the distribution of the difference in alpha modulation during EO and EC blocks. More specifically, we used a protocol analogous to that for extracting alpha ERD to estimate alpha power during EO and EC conditions. We found the mean within each condition at the group spectral peak of alpha power, and calculated the difference between EO and EC across electrodes. The mean modulation values from all 256 electrodes were plotted on a scree plot and the maximal response electrodes were identified by finding the elbow in the scree plot, identifying a total of 29 electrodes (E96, E97, E106, E107, E108, E109, E114, E115, E116, E117, E118, E124, E125, E126, E136, E137, E138, E139, E148, E149, E150, E151, E152, E159, E160, E161, E168, E169, E170) that corresponded with an occipital topography (see Fig. 3c). The mean alpha ERD amplitudes were analyzed using repeated-measures ANOVA and/or t-tests for effects of GROUP, LOAD and their interaction. Additionally, for *EEG-fMRI analyses*, single-trial values for alpha ERD were extracted, as discussed below.

Finally, we performed additional analyses to identify outliers based on EEG data, which are susceptible to both effects of motion and residual BCG artifacts. We therefore identified participants who had <10 correct trials following all cleaning steps, and those who were outliers in mean ERSP spectral power below alpha (<7 Hz), in which BCG effects (outside of the alpha ERD) tend to be expressed maximally. This analysis identified 9 participants whose data was unsuitable for further analyses (Inline Supplementary Fig. S1), as discussed in more detail below. Remaining participants had on average 40 epochs remaining, following all cleaning steps, for use in the *EEG-fMRI analyses* (ADHD: $M = 38$, $SE = 3.2$; TD: $M = 42$, $SE = 2.1$).

Inline Supplementary Fig. S1 can be found online at http://dx.doi.org/10.1016/j.nicl.2016.01.023.

2.4.5. EEG-fMRI analyses

We used a psychophysiological interaction (PPI) analysis (Friston et al., 1997; McLaren et al., 2012) to identify the activity and connectivity associated with alpha ERD across groups. This analysis was conducted using FSL software, and an approach analogous to the *fMRI localizer analysis*. However, the general linear model included not only event and nuisance regressors, but also PPI-related regressors. Namely, we included nine event regressors to model: accurate-trial encoding, maintenance and to probe events at each LOAD, as well as inaccurate-trial encoding, maintenance and probe events. The encoding regressors were used to quantify activation during encoding, as well as effects of GROUP, LOAD and their interaction. We also included two nuisance regressors: the timeseries of ventricle and white matter amplitude changes across block. Finally, the three additional PPI regressors included a regressor of event-related alpha ERD (c.f. *EEG Preprocessing*) for all accurate trials, the time series of an ROI (either rOccLat, rOccS, or rFEF), and an interaction term between alpha ERD and the time series of an ROI (c.f. *fMRI localizer analyses*). As we identified three ROIs in the *fMRI localizer analysis*, the analysis was performed for each ROI separately. The PPI term in each of these analyses was constructed by multiplying the alpha ERD regressor by the deconvolved timeseries of the ROI (Gitelman et al., 2003), and reconvolving the product with the hemodynamic response function. Thus, the alpha ERD regressor was used to identify regions that covaried in activation with changes in alpha ERD, whereas the PPI term was used to identify regions whose functional connectivity with the ROI in question varied with magnitude of alpha ERD. Both effects in this model represent alpha ERD activity and connectivity changes independent of the main effects of encoding, maintenance and response to probe during the task.

As for *fMRI localizer analysis*, we assessed significance at the group-level, for each regressor, using a mixed-effects model. We included contrasts for assessment of mean regressor significance across all participants, thresholded using cluster detection statistic, with a height threshold of $z > 2.3$ and cluster probability of $p < 0.05$, and corrected for whole-brain multiple comparisons using Gaussian random field theory. We then used ANOVAs to assess effects of GROUP within each regressor, alpha ERD activity and functional connectivity, result. Note that because we modeled alpha ERD as a continuous variable across all trials, we do not test for LOAD effects in the alpha ERD related effects. However the inclusion of alpha ERD as a regressor in the model, in addition to the interaction term (alpha ERD x ROI timeseries), ensures that the load effect is modeled. We additionally calculated partial correlations between regression coefficients for alpha ERD and alpha ERD PPI effects and performance (RT, RTsd, accuracy), and symptoms. All reported partial correlation analyses were assessed statistically at $p < .05$, two-tailed unless stated otherwise, and were performed on residuals following removal of *age* from each variable in order to account for developmental effects within the sample.

3. Results

3.1. Sample demographics and performance

The sample demographics are presented in Table 1. The outlier analysis identified 9 participants whose EEG data was insufficient for analysis. The demographic and performance statistics highlight important differences between the full sample (n = 30) and the reduced sample (n = 21). The excluded subjects were significantly younger, $t(28) = 2.5$, $p < .02$, (13.2 yrs. vs. 14.2 yrs), and had significantly higher inattention, $t(28) = 2.6$, $p < .02$, (9 vs. −5.3) and hyperactivity, $t(28) = 3.7$, $p < .001$, (6.3 vs. −12.5) symptom SWAN scores than the included subjects, consistent with the fact that 7 out of 9 excluded subjects had ADHD. We suspected that this occurred because of excessive motion in these participants. Analysis of fMRI motion parameters confirmed that the excluded subjects had significantly greater motion of the head, both in rotation, $t(28) = 1.8$, $p < .08$, (.24 vs. .04), and translation, $t(28) = 3.1$, $p < .004$, (10.1 vs. 1.7). Furthermore, a focused analysis of ADHD participants indicated that the 7 excluded subjects had greater hyperactivity symptoms, $t(28) = 2.9$, $p < .01$, (11.1 vs. −.3), and were more likely to be diagnosed with combined type ADHD, $\chi^2(1, N = 15) = 3.2$, $p < 0.07$, than the 8 included subjects. These results clearly demonstrate that head motion contributed to corruption of our EEG data, and also that our reduced, final sample comprised primarily inattentive-type ADHD participants (6/8).

Within the reduced sample, the ADHD and TD groups did not differ in mean age, $t(19) < 1$, (ADHD: 14.1 yrs., TD: 14.3 yrs) or FSIQ, $t(19) = 1.2$, $p < .23$, (ADHD: 105, TD: 112), or WRAT scores, $t(19) = 1.2$, $p < .26$, (ADHD: 124, TD: 115), indicating no differences in IQ or verbal learning ability. Participants with ADHD did show significantly higher ratings of SWAN symptoms (suggesting worse functioning), both inattentive, $t(19) = 4.6$, $p < .001$, (ADHD: 7.3, TD: −13.1), and hyperactivity, $t(19) = 5$, $p < .001$, (ADHD: −.3, TD: −20.1), consistent with the diagnoses. As expected based on our outlier analysis the ADHD hyperactivity score was near zero ($M = .3$, $SE = 2.8$). Notably the groups did not differ in performance on the SWM task, in accuracy, RT or RTsd, during either practice or scanning, $F(1,19) < 1.2$. During the scanning session, we

Table 1
Sample demographics, symptoms, and performance.

	N	Age (y)	FSIQ	$SWAN_{inatt}$	$SWAN_{hyper}$	WRAT	Scan performance			Prep performance		
							Acc	*RT (s)*	RT_{sd}	*Acc*	*RT (s)*	RT_{sd}
$N = 30$												
ADHD	15	13.7	104	10.7*	5.1*	113	.75	1.2	.49	.77*	1.3	.43
TD	15	14.1	111	−12.7*	−18.8*	123	.80	1.1	.43	.88*	1.2	.37
$N = 21$												
ADHD	8	14.1	105	7.3*	−0.3*	115	.80	1.1	.43	.82	1.2	.38
TD	13	14.3	112	−13.1*	−20.1*	124	.82	1.1	.45	.89	1.2	.38

FSIQ, full-scale IQ; *SWAN*, Strengths and Weaknesses of ADHD symptoms and Normal Behavior Scale with (*inatt*) inattentive and (*hyper*) subscales (higher SWAN scores indicate worse functioning); *WRAT*, wide range achievement test (verbal); *Acc* accuracy; *RT/sd* reaction time and its standard deviation; *SCAN* fMRI-session; *PREP* pre-fMRI session.
* $p < .01$ significant group difference.

found a significant effect of LOAD indicating that performance was worse when encoding 5 dots than when encoding 1 dot for accuracy, $F(1,19) = 47.7$, $p < .001$ (1-dot: 87%, 5-dot: 73%), RT, $F(1,19) = 73.9$, $p < .001$ (1-dot: 1.0 s, 5-dot: 1.3 s) and also RTsd, $F(1,19) = 3.1$, $p < .09$ (1-dot: .36 s, 5-dot: .42 s). Effects of LOAD did not interact with GROUP, $F(1,19) < 1$. These findings are consistent with previous reports of load effects on SWM performance but also indicate that our sample of children with ADHD performed comparably to TD children.

3.2. fMRI activation analyses

The activation responses to encoding stimuli and to dot stimuli during the stimulus localizer (Fig. 2) were similar, supporting the use of the localizer scan for priors on ROIs for the connectivity analyses. Both analyses revealed activation of right inferior lateral occipital cortex, bilateral superior occipital cortex and right frontal eye fields, consistent with expected involvement of fronto-parietal regions in visuospatial processing. For the encoding events during SWM there was no significant effect of GROUP, nor an interaction of GROUP with LOAD. The LOAD effect was evident only in left inferior lateral occipital cortex (x = −24 mm, y = −94 mm, y = 8 mm; 437 voxels, z = 3.01), likely reflecting an elevated visual response with more visual stimuli (5 dots vs. 1 dot) on screen. A contrast comparing the encoding and stimulus localizer conditions revealed stronger activation (i.e., significantly greater z-scores) in the localizer relative to the encoding events, consistent with the more powerful block design used, but no differences in activation pattern. There were no significantly greater activations during encoding events relative to the localizer, suggesting that the same regions show BOLD signal increases when viewing and encoding the visual dot stimuli. No GROUP effects were present in the localizer response, nor in the difference between localizer and encoding activations. Based on this analysis we therefore selected the cluster peaks for rOccLat, rOccS and rFEF (Fig. 2 and Table 2) as ROIs for the subsequent PPI connectivity analyses. Left OccS showed results analogous to its right homologue and is thus not further reported.

3.3. Alpha ERD analyses

We observed reliable alpha ERD during encoding in both groups (Fig. 3, Inline Supplementary Fig. S2), maximally distributed over occipital electrodes as expected, and consistent with locations of electrodes identified a priori using the EO/EC localizer condition (Fig. 3c). Alpha ERD was significantly greater, $F(1,19) = 6.2$, $p < .02$, at higher load (5-dot, −2.61 dB) than at low load (1-dot: −2.23 dB), and showed a trend effect of GROUP, $F(1,19) = 2.8$, $p < .1$. Consistent with our prior report, alpha ERD was greater in the TD group (−2.89 dB) than in the ADHD group (−1.95 dB). The interaction was not significant, $F(1,19) = 1.1$, $p < .3$.

Inline Supplementary Fig. S2 can be found online at http://dx.doi.org/10.1016/j.nicl.2016.01.023.

To validate that the alpha ERD collected during fMRI captured the between group variability in our participants outside of fMRI, we correlated alpha ERD across practice and scanning sessions. The correlation was significant, $r(19) = .6$, $p < .01$ (see Fig. 3e). We thus also repeated the group analysis in the practice data set, taking advantage of the full sample size (n = 30, i.e., there were no exclusions in the EEG-only data). In the larger sample the two-sided group difference approached significance, $t(28) = 1.87$, $p < .07$ (ADHD: −1.73 dB, TD: −3.49 dB). The alpha ERD group difference was thus replicated, and stronger with increasing sample size. The effect size for this group difference was large in both practice (Cohen's $d = .7$) and scanning (Cohen's $d = .79$) sessions.

3.4. EEG-fMRI analyses: neural correlates of alpha ERD

We conducted three PPI analyses, to assess alpha ERD activity and connectivity for each of rOccLat, rOccS, and rFEF. These analyses

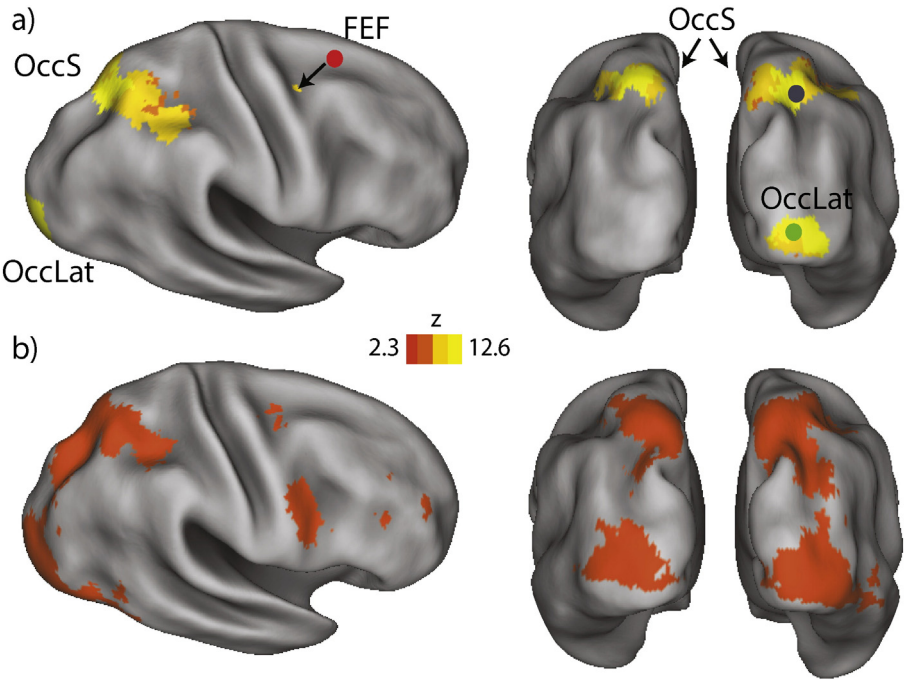

Fig. 2. fMRI activation results. The stimulus localizer (a) elicited activation responses in lateral occipital (OccLat) and superior occipital (OccS) cortices, as well as right frontal eye fields (FEF). Red (FEF), black (OccS), and green (OccLat) dots indicate locations of regions of interest used in PPI analyses. Similar activation was elicited by the encoding stimulus (b) during the SWM task. The stimulus localizer activation patterns showed a larger effect size, higher z-scores, but no other differences were significant between localizer and encoding conditions. Parametric maps thresholded at cluster height of $z > 2.3$, $p < .05$, whole-brain corrected for multiple comparisons.

Table 2
Cluster statistics.

		x (mm)	y (mm)	z (mm)	#Voxels	Max Z
Stimulus localizer: activity increases						
Right (& left) occipital cortex, superior	RL OccS	26	−62	52	1385	11.7
Right lateral occipital cortex, inferior	R OccLat	20	−94	2	438	13.5
Right frontal eye fields (pre-central gyrus)	R FEF	32	−4	46	10	7.63
Alpha ERD: activity increases						
Right lateral occipital cortex, inferior	R OccLat	32	−98	−4	1105	2.84
Left lateral occipital cortex, inferior	L OccLat	−32	−86	−4	1584	3.07
Alpha ERD: activity decreases						
Right (& left) planum temporale/parietal operculum	RL PT/PO	56	−34	22	6261	3.21
Left post-central gyrus	R postCG	−52	−22	52	4504	3.16
Right (& left) lingual gyrus	RL Lingual	2	−76	6	1605	2.82
Right (& left) superior frontal gyrus extending into paracingulate gyrus	RL rSFG/paraCG	4	36	44	1404	2.81
*Alpha ERD * rOccS: connectivity increases*						
Right lateral occipital cortex, superior	R OccS	18	−68	64	343	3.26
*Alpha ERD * rFEF: connectivity increases*						
Right frontal pole	R FP	28	50	28	388	3.06
Right frontal operculum; inferior frontal gyrus	R iFG	46	14	−2	311	2.98
Left frontal operculum; inferior frontal gyrus	L iFG	−48	14	−2	312	3.38
Superior parietal lobule; precuneuous cortex	sPL	−2	−46	66	421	2.92
*Alpha ERD * rOccLat: connectivity increases*						
Right superior parietal lobule; post-central gyrus	R SPL/postCG	40	−36	50	426	2.80
Right lateral occipital cortex superior	R OccS	8	−76	52	361	3.04
Right pre-central gyrus	R preCG	40	−4	54	345	2.92
Left superior temporal gyrus	L sTG	−56	−22	−4	270	2.99

Note. Cluster centroids are reported at maximum statistic. Statistic for bilateral effects reported for hemisphere with maximal statistic; medial clusters span across hemispheres.

revealed a consistent effect for alpha ERD on neural activity (Fig. 4), as well as significant connectivity changes (Fig. 5), within a fronto-parieto-occipital network. Both of these effects differentiated between TD and ADHD participants.

3.4.1. Alpha ERD & neural activity

Since the alpha ERD regressor was common to all three ROI analyses (rOccLat, rOccS, rFEF), we present here the union across the three analyses. As shown in Fig. 4 (and in Table 2), greater alpha ERD (i.e., more negative power change) during encoding was accompanied by increases of activity in lateral occipital cortex and occipital pole bilaterally, consistent with prior reports. Notably, this negative relationship was stronger in the TD ($\beta_z = -11.3$) group than in ADHD ($\beta_z = -3.5$), $F(1,19) = 3.8$, $p < .06$ (Cohen's $d = .88$). Furthermore, decreases in BOLD signal with enhanced alpha ERD were observed across sensorimotor regions including planum temporale, pre- and post-central gyri, lingual gyrus and medial frontal cortex, but this effect did not differ across groups, $F(1,19) < 1$, (ADHD: $\beta_z = 6.7$, TD: $\beta_z = 6.1$, Cohen's $d = .11$). Finally we tested if alpha ERD effects on neural activity predicted either performance or symptoms. We found no significant relationship between alpha effects on activation and RT, RTsd, accuracy or SWAN scores, $p > .17$, $r(19) < .31$. In sum, the ADHD group showed weaker occipital activation with alpha ERD than the TD group. It is notable however that alpha ERD was non-zero in the ADHD group ($M = -1.95$ dB, $SE = .45$ dB), and was both non-zero and did not differ among groups in positive correlations with neural activity (Fig. 4b). Thus alpha ERD was likely associated with a *different* process, rather than being absent in ADHD participants. One alternative explanation is discussed below.

3.4.2. Alpha ERD & network functional connectivity

The network correlates of alpha ERD are shown in Fig. 5 (and in Table 2). All three ROIs exhibited a significant negative interaction term, reflecting more positive connectivity with greater alpha ERD (i.e., more negative alpha power). The connectivity of the rFEF ROI with fronto-parietal regions (right frontal pole, bilateral inferior frontal gyrus and medial superior parietal lobule) increased with greater alpha ERD. This effect was significantly $F(1,19) = 8.8$, $p < .01$ (Cohen's $d = 1.4$), stronger in ADHD ($\beta_z = -2.9$) than in TD ($\beta_z = -1.1$) participants. Similarly, with greater alpha ERD, the rOccLat ROI was more strongly connected with a set of more posteriorly distributed fronto-parietal regions (right superior parietal lobule and right superior occipital cortex, right pre-central gyrus) as well as right superior temporal cortex. Again, this effect was greater $F(1,18) = 25.9$, $p < .001$ (Cohen's $d = 2.5$), in ADHD ($\beta_z = -3.1$) than in TD ($\beta_z = -.9$) participants (we removed one TD participant from this analysis due to an outlier value in the fMRI result). Thus alpha ERD *connectivity*, seeded by rFEF and rOccLat, with a network of fronto-parieto-occipital regions was stronger in ADHD than in TD participants, in contrast to the group effect for alpha ERD associated occipital activity.

The rOccS ROI, however, revealed a rather limited connectivity profile, stronger connectivity with nearby right lateral occipital cortex regions, with stronger alpha ERD, and this effect did not differ by group, $F(1,19) = 1$, $p < .33$ (Cohen's $d = .5$), (ADHD: $\beta_z = -2.4$, TD: $\beta_z = -1.6$). Given the proximity of this area to the ROI itself, and the spatial extent of the smoothing kernel (5 mm) that we used in preprocessing of the data, it is possible that this effect was partly artifactual. Yet the connectivity result for the rOccS overlapped with connectivity of rOccLat (Fig. 5), suggesting that this region may be a node of that network. To explore this further we examined the connectivity patterns at a lower, whole-brain corrected, threshold ($z > 2$) (Inline Supplementary Fig. S3, Inline Supplementary Table S1), and confirmed that the spatial extents of the three networks associated with rFEF, rOccS, and rOccLat overlap considerably. Thus it is prudent, until further data suggests otherwise, to interpret the three ROI networks as the most reliable subsets of a greater fronto-parieto-occipital network, rather than as three separate networks. It is possible, consistent with the medium effect size of the rOccS group effect, that the connectivity of this region will show a reliable group difference in a larger sample as part of this larger network.

Inline Supplementary Fig. S3 and Table S1 can be found online at http://dx.doi.org/10.1016/j.nicl.2016.01.023.

We tested also if the effect of alpha ERD on connectivity of rFEF, rOccS and rOccLat predicts performance on the SWM task or total ADHD symptoms. The relationship between alpha ERD connectivity

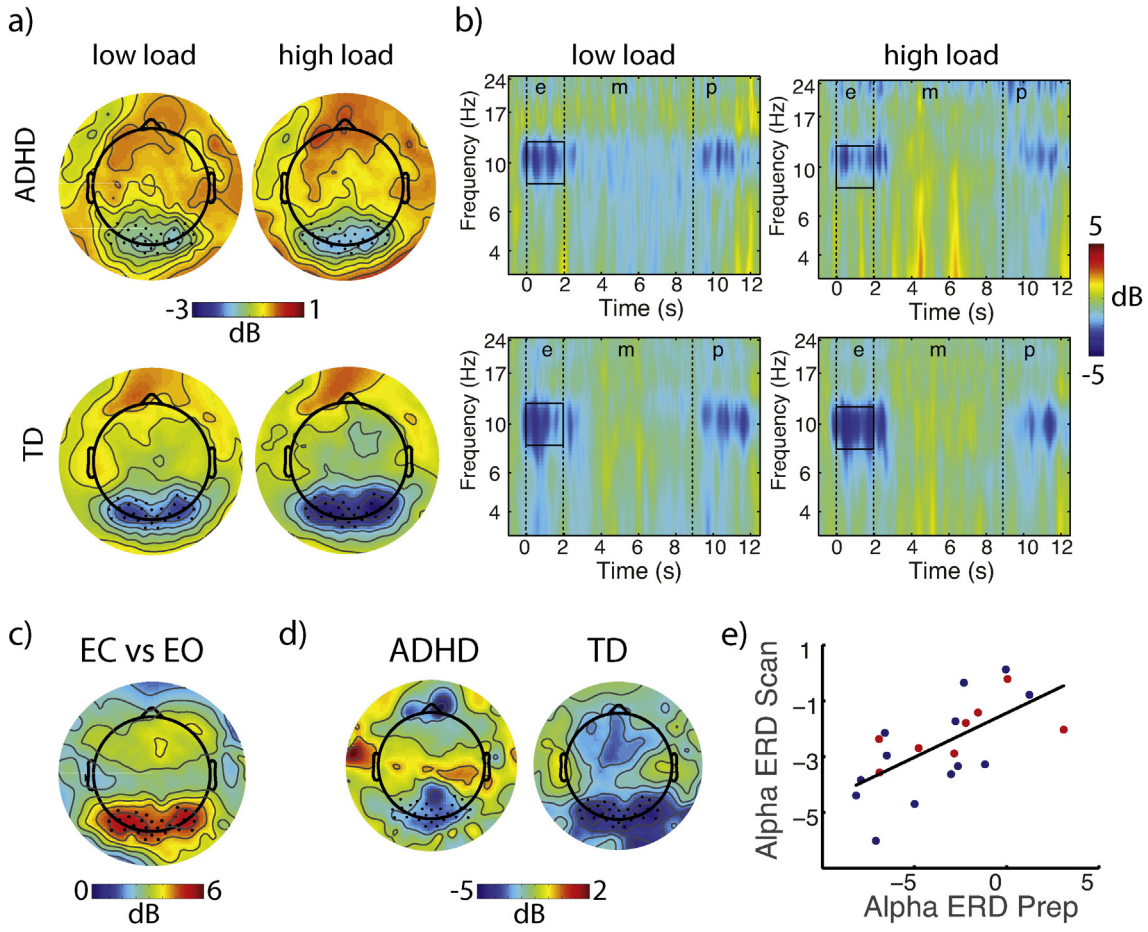

Fig. 3. Alpha ERD EEG Results. Alpha ERD during SWM encoding (a,b) performed during fMRI was observed in both ADHD and TD participants, was distributed spatially over occipital electrodes (a) and temporally throughout the 2 s encoding interval (b). Alpha ERD was greater for higher load and in TD participants. A comparison of peak alpha power during pre-scan eyes-open (EO) and eyes-closed (EC) conditions (c) was used to identify electrodes of interest for alpha ERD analyses. Alpha ERD was also weaker in ADHD than in TD participants during preparatory practice (d), pre-scanning, and was significantly correlated with alpha ERD during scanning (e), indicating that between-subject variability was preserved in the concurrent EEG-fMRI recordings. TD, typically developing; ADHD, attention deficit hyperactivity disorder; ERD, event-related desynchronization.

and performance was not significant for any of the ROIs, $r(19) < |.26|$, $p > .25$. However, alpha ERD connectivity for rOccLat was correlated significantly with SWAN symptoms (Fig. 6, middle plot), $r(18) = -.6$, $p < .005$, indicating that those individuals with the strongest increase in rOccLat connectivity with alpha ERD also had the most severe ADHD symptoms, consistent with the direction of the group effect. The same correlations were not reliable for rOccS, $r(19) = -.2$, $p < .4$, or rFEF, $r(19) = -.35$, $p < .12$.

3.4.3. Network connectivity and performance

The absence of a relationship between either alpha ERD related activation, or connectivity, and performance prompted us to investigate additionally if the connectivity with identified networks, independent of their relationship to alpha ERD, predicted performance. That is we wondered if the correlates of alpha ERD versus network strength are measures of different dimensions of the experiment (ADHD symptoms and task performance, respectively). We thus estimated connectivity for each network in the full sample (n = 30) and tested the one-sided hypothesis that stronger fronto-parietal connectivity during encoding would be associated with better performance. The results (Fig. 7) show that for all three ROIs, stronger network connectivity was associated with faster and less variable response times: rFEF: $r_{RT}(28) = -.38$, $p_{RT} = <.02$ and $r_{RTsd}(28) = -.38$, $p_{RTsd} = <.02$; rOccS: $r_{RT}(28) = -.32$, $p_{RT} = <.04$ and $r_{RTsd}(28) = -.29$, $p_{RTsd} = <.05$; rOccLat: $r_{RT}(28) = -.31$, $p_{RT} = <.05$ and $r_{RTsd}(28) = -.33$, $p_{RTsd} = <.04$. The stronger connectivity of rOccS also was associated with higher accuracy, $r(28) = .39$, $p < .02$. No ROIs showed a relationship between connectivity and ADHD symptoms, $r(28) < .27$, $p > .14$, in contrast to the alpha ERD related effects. Thus connectivity and performance were related, but overall network connectivity did not predict group differences or symptoms. Finally, we evaluated if network *connectivity* differed by group, and found no significant effects. The combined results indicate that the portion of variance of functional connectivity within the fronto-parieto-occipital network associated with alpha ERD, was predictive of group differences and symptoms, whereas the overall connectivity was predictive of RT and RT_{sd}, and less so of accuracy.

4. Discussion

Our study objectives were to test if encoding-related alpha ERD correlates with fronto-parieto-occipital connectivity, whether this is further disrupted in ADHD, and whether it predicts symptoms or performance in SWM. The results indicate that alpha ERD during SWM encoding was associated with *both* occipital activation and fronto-parieto-occipital functional connectivity, thus expanding on prior associations between alpha ERD and occipital activation. This finding provides novel support for the interpretation of alpha ERD as a modulatory effect that involves, and perhaps arises as a result of, top-down network interactions. The group analyses revealed attenuated occipital activation and enhanced fronto-parieto-occipital connectivity correlates of alpha ERD in children with ADHD relative to their TD peers. Alpha ERD and its relationship to fronto-parieto-occipital connectivity

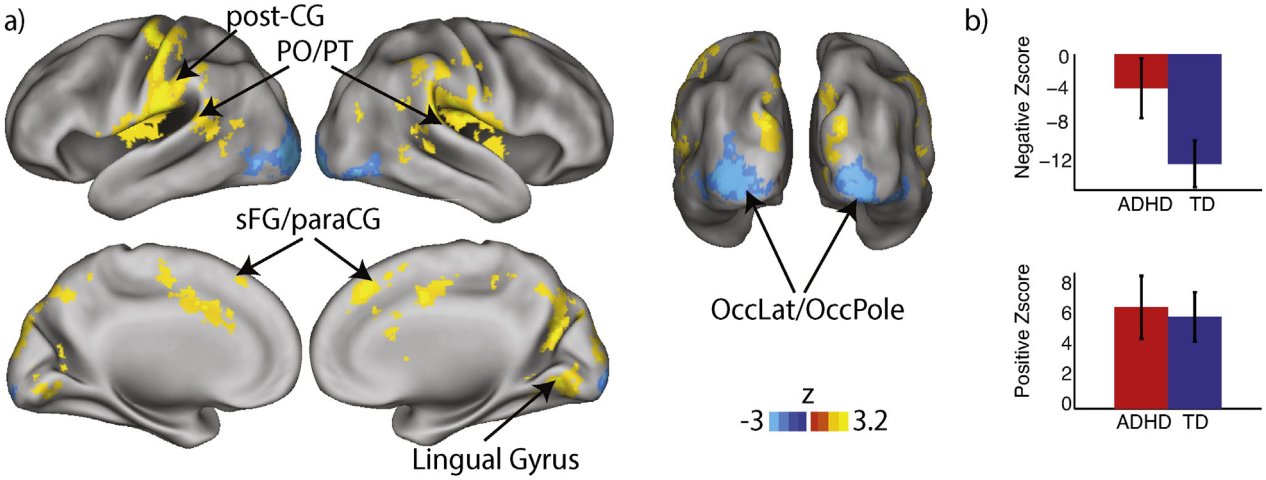

Fig. 4. EEG-fMRI results: alpha ERD & neural activity. Greater alpha ERD during SWM encoding predicted (a) increases of activity in bilateral lateral occipital cortex (OccLat) and occipital pole (OccPole), and with decreases of activity in post-central gyrus (post-CG), planum temporale (PT), posterior operculum (PO), and superior frontal gyrus (sFG) extending into paracingulate cortex (paraCG). The mean activation effect across occipital cortices was significantly stronger in the TD group than in the ADHD group (b, top), whereas the group difference was not significant for the activation decreases associated with alpha ERD (b, bottom). TD, typically developing; ADHD, attention deficit hyperactivity disorder. Parametric maps thresholded at cluster height of $z > 2.3$, $p < .05$, whole-brain corrected for multiple comparisons.

correlated with inattention symptoms. The interpretation of the group differences must be considered in light of the small sample size of the study, strongly affected by participant motion, enhanced in those with hyperactive symptoms. Our results provide a first, concurrent EEG-fMRI characterization of alpha ERD and its network correlates in children, and outline both limitations and possible solutions when applying the methodology to hyperkinetic populations, such as combined type ADHD.

4.1. Neural correlates of alpha ERD

The functional mechanisms of alpha ERD, and of ERS, in visual perception and attention have been discussed extensively, with prominent theoretical accounts suggesting that event-related modulation of alpha power reflects processes that regulate information flow in the cortex via selective suppression and selection of sensory signals (Foxe and Snyder, 2011; Klimesch, 2012; Klimesch et al., 2007; Palva and Palva, 2007). For

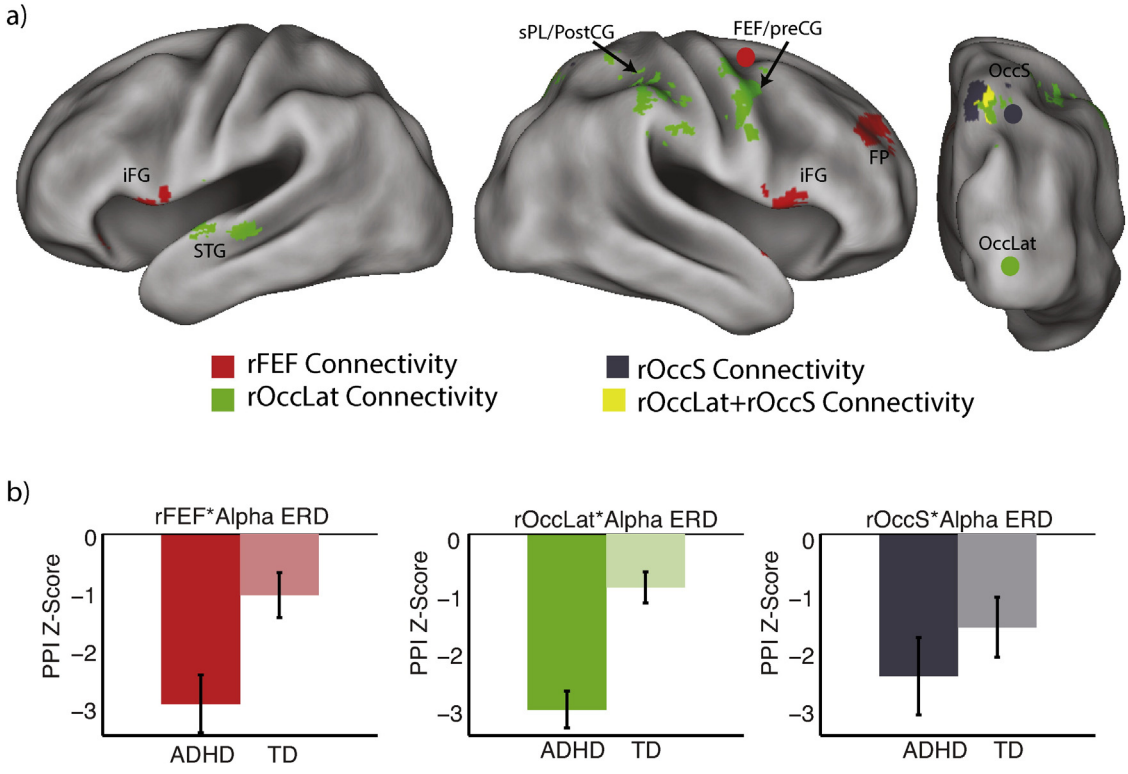

Fig. 5. EEG-fMRI results: alpha ERD & network connectivity. Greater alpha ERD during SWM encoding predicted (a) increased functional connectivity between right frontal eye fields (rFEF, red) and bilateral inferior frontal gyri (iFG), and frontal pole (FP); increased functional connectivity between right lateral occipital cortex (rOccLat, green) and post- and pre-central gyri (post/pre-CG), superior parietal lobe (sPL) and superior temporal gyrus (sTG); increased functional connectivity between superior occipital cortex (sOcc, gray) and surrounding regions, which overlapped (yellow) with the connectivity of rOccLat. The connectivity increase associated with alpha ERD was greater in ADHD (b) for both rFEF and rOccLat regions of interest, but not for rOccS. TD, typically developing; ADHD, attention deficit hyperactivity disorder. Parametric maps thresholded at cluster height of $z > 2.3$, $p < .05$, whole-brain corrected for multiple comparisons.

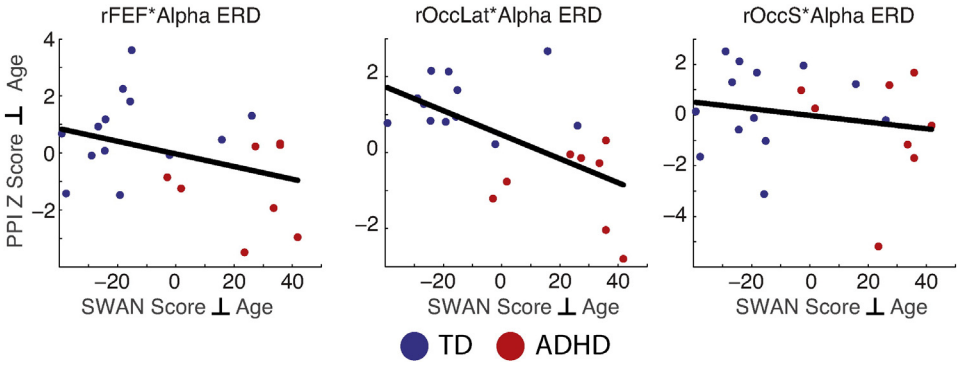

Fig. 6. Alpha ERD connectivity & symptoms. The association of the right occipital lateral (rOccLat) network with alpha ERD, predicted greater ADHD symptoms (middle), $r(18) = -.6$, $p < .01$, indicating a dissociation between groups in the same direction as the group effect in the PPI. The same effect was not reliable for right frontal eye field (rFEF) and right superior occipital (rOccS) regions of interest. TD, typically developing; ADHD, attention deficit hyperactivity disorder; SWAN, strength and weaknesses of ADHD symptoms and normal behavior rating scale. Plotted are residuals of each variable regressed on participant age, thus removing effects of development from the analyses.

instance, attention to a visual dimension such as left or right visual space, results in a decrease of alpha power in contralateral visual cortex and an increase in alpha power in cortical regions corresponding to the unattended dimension. Furthermore these modulations reflect increases and decreases, respectively, of cortical excitability (Chaumon and Busch, 2014; Lange et al., 2013; Romei et al., 2008), providing strong evidence that within sensory cortex, alpha ERD captures the effects of associative networks.

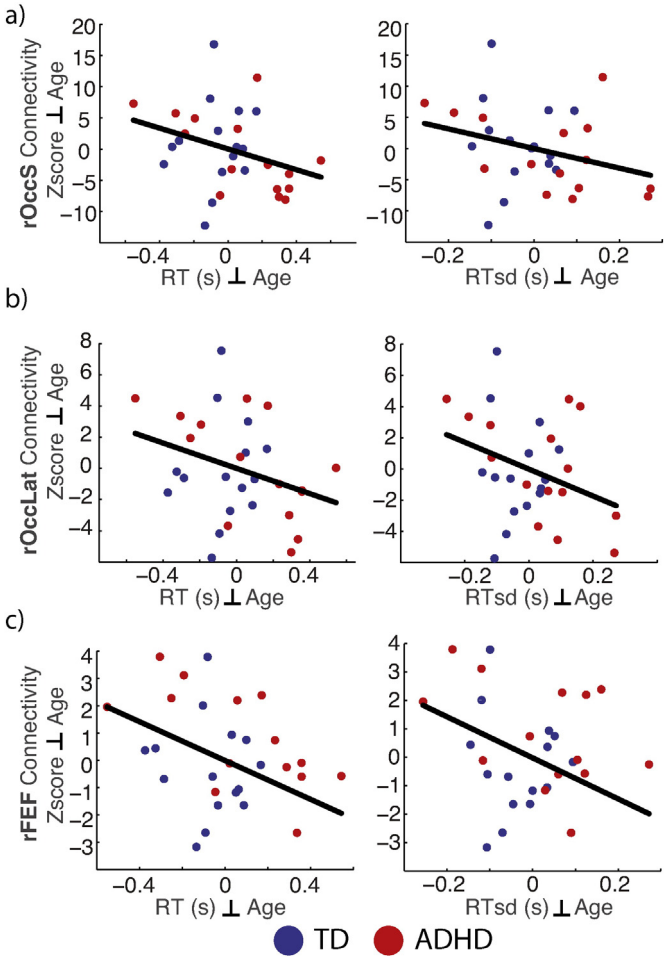

Fig. 7. ROI connectivity & performance. Independent of the association with alpha ERD, greater connectivity of right superior occipital (rOccS) (a), right lateral occipital (rOccLat) (b), and right frontal eye fields (rFEF) (c), predicted faster (left column) and less variable (right column) response time (RT) on the task, indicating a role for these networks in task performance. Note that unlike the effects of alpha ERD the connectivity and performance metrics do not differ across groups. TD, typically developing; ADHD, attention deficit hyperactivity disorder. Plotted are residuals of each variable regressed on participant age, thus removing effects of development from the analyses. RT, reaction time; RTsd, reaction time standard deviation.

The present study expands on these findings by showing that alpha ERD may also capture the connectivity of such associative networks, and this connectivity predicts task performance. This idea, though a natural extension of existing literature, has not been tested previously using EEG-fMRI (see Scheeringa et al., 2012 for a related analysis of connectivity within visual cortex and alpha fluctuations during rest), but has been elaborated on by Palva and Palva (2007, 2011), on the basis of neurophysiological analyses of long-range synchrony among sensori-fronto-parietal regions within the alpha frequency band during complex cognitive operations such as WM. Of note, alpha ERD need not be associated exclusively with sensori-parieto-frontal network activity, which may be specific to the top-down influences in the SWM paradigms used by us and by Palva and Palva (2007, 2011). Klimesch (2012), based on data from an array of spatial and non-spatial experiments, made a strong argument that modulation of alpha power can reflect a variety of higher order operations that might contribute to modulation of sensory signals, including categorization, semantic analysis, and memory retrieval. Thus the identity of the alpha-correlated network may vary with the functional demands of the task.

The relationship between alpha power decrease and increased *occipital activity* has been documented thoroughly in spontaneous recordings of alpha in humans (Busch et al., 2009; de Munck et al., 2007; Goldman et al., 2001; Laufs et al., 2003; Moosmann et al., 2003; Romei et al., 2008; Wyart and Tallon-Baudry, 2009), as well as in intracortical recordings in animal models (Bollimunta et al., 2008; Bollimunta et al., 2011; Lopes da Silva, 1991; Mo et al., 2011), cementing the link between alpha power and cortical responsiveness to visual stimuli. Our findings of such a relationship during encoding therefore are consistent with prior accounts, as well as with dipole localization results that we reported previously in this task (Lenartowicz et al., 2014). However, reports of positive correlations between alpha power and cortical activity are more variable. Most commonly, positive correlations with alpha power have been reported in thalamus (de Munck et al., 2007; Goldman et al., 2001; Goncalves et al., 2006; Luchinger et al., 2011; Luchinger et al., 2012; Moosmann et al., 2003). One exception is Liu et al. (2014) who reported positive correlations with alpha power in core regions of default mode network (middle temporal gyrus and medial prefrontal cortex) and sensorimotor cortices. Our present findings are consistent with those of Liu et al. (2014) as we observed positive correlation of alpha ERD in primary sensorimotor cortices (pre- and post-central gyri and auditory cortex) as well as medial frontal cortex, with no effect in thalamus. A prominent difference between the two sets of findings, the thalamic activations were reported in studies of spontaneous alpha power fluctuations,

whereas the study of Liu et al. (2014) as well as the current study, examined alpha in response to an attention-orienting cue and encoding stimulus, respectively. The difference between spontaneous and attention generated modulations in alpha power may be related directly to underlying mechanisms. As alpha power can be modulated through either thalamo-cortical interactions or through cortico-cortical interactions (Lopes da Silva, 1991; Lopes da Silva et al., 1980), it is conceivable that the former mechanism is dominant in spontaneous recordings whereas both mechanisms may contribute to modulations in task-based studies of alpha power, such as ours and that of Liu et al. (2014). In light of the known attentional effects on alpha, the positive correlations we report may represent attentional suppression of regions that are not involved in encoding.

4.2. Alpha ERD neural correlates in ADHD

We identified two key differences in children with ADHD relative to TD peers: weaker alpha ERD relationship to occipital activity, but stronger relationship with fronto-parieto-occipital connectivity. A parsimonious account of the former effect, in light of the discussed mechanisms of alpha ERD is that in children with ADHD occipital modulation during encoding was weaker due to a weaker attention effect. In complement, the enhanced connectivity within a fronto-parieto-occipital network during alpha ERD in the ADHD sample may be a compensatory response. However, this account must be tempered by data suggesting that attentional processes that rely on fronto-parietal connectivity, including visual orienting (Huang-Pollock and Nigg, 2003; Huang-Pollock et al., 2006; Nigg et al., 1997; Oberlin et al., 2005), load effects (Friedman-Hill et al., 2010; Huang-Pollock et al., 2002; Lenartowicz et al., 2014), and visual search (Mason et al., 2005; Mason et al., 2003) do not show group differences, which speaks against a uniform deficit in the fronto-parietal network. If such a deficit exists, and fMRI studies do support frontal–parietal deficits in ADHD (e.g., see Cortese et al., 2012 for a review), it may be dependent on yet-to-be determined contextual factors. An interesting possibility arises from a recent finding by Stevens et al. (2012) who demonstrated a perceptual interference deficit in adults with ADHD in the absence of a spatial attention deficit. By using a luminance-threshold outcome measure they showed that adults with ADHD were more susceptible to the presence of visual distractors, but had preserved attentional responses to cuing. This finding shifts the source of the attentional modulation deficit from top-down fronto-parietal networks, to bottom-up visual cortex processing, or perhaps the ability of visual cortex to "respond to" top-down signals. This could, for instance, correspond to neuromodulatory mechanisms within occipital cortex, in particular those that are responsible for lateral inhibition, or visual cortex connectivity (e.g., Scheeringa et al., 2012). Thus the stronger relationship between alpha ERD and fronto-parieto-occipital connectivity in ADHD may indeed reflect a compensatory response but due to poor implementation of modulation within occipital cortex. This hypothesis remains to be tested. Notably, we are not aware of prior findings of alpha-related functional connectivity in ADHD, with the exception of Mazaheri et al. (2010, 2013) who report on spectral power correlations between occipital and frontal electrodes in ADHD, a finding that, because of the lack of direct correspondence between electrodes and underlying cortical sources, does not directly assess functional connectivity of the neural generators of alpha ERD.

More broadly, our data do not support a deficit localized to WM processes of maintenance, which likely includes frontal activities mediated by dopaminergic signals. Because encoding-related deficits necessarily precede maintenance, participants who show such a deficit must be subject to attentional problems that are independent of WM maintenance. This also may explain why stimulants that target dopaminergic and noradrenergic function within these systems, thought to underlie maintenance, are inconsistent in their therapeutic effects (Rubia et al., 2013, 2014). Interestingly, the pattern of results that we report here also is consistent with a vigilance deficit in ADHD (Huang-Pollock et al., 2012; Huang-Pollock et al., 2006; Sergeant, 2005), yet another external system necessary for effective performance of a WM task, since poor vigilance could also result in weak occipital modulation and compensatory fronto-parieto-occipital engagement. Accordingly, we have demonstrated previously that in the same SWM task participants with ADHD, in addition to weaker alpha ERD, had a weaker response to the alerting cue that preceded the encoding stimulus (Lenartowicz et al., 2014). Finally, our ADHD participants did not differ from TD peers in *positive* correlations between alpha ERD and neural activity. Positive correlations with alpha ERD correspond to regions that decrease in activation during occipital activation and thus may, as discussed in the prior section (also Liu et al., 2014), reflect inhibitory attentional modulation. If so, attentional suppression, a top-down function, was not impaired reliably in our ADHD sample, in contrast to the attentional enhancement associated with alpha ERD. This observation is broadly consistent with both the perceptual interference and vigilance accounts of ADHD deficits in attention.

An important caveat to the interpretation of our results is the unforeseen bias in the ADHD sample to primarily inattentive type subjects. This bias occurred because 5/7 of ADHD subjects, excluded primarily due to motion, had combined or hyperactive type ADHD diagnosis (versus 2/8 of included ADHD subjects). The outlier sample was more likely to show hyperactive diagnosis, $\chi^2(1,n = 15) = 3.2$, $p < .07$, and symptoms, $t(13) = 2.9$, $p < .01$. Thus we cannot claim that the present findings extend to combined/hyperactive type ADHD, and may be representative only of inattentive type ADHD. This possibility is consistent with prior data. In a larger sample, we have found (Lenartowicz et al., 2014) that alpha ERD was correlated significantly with inattentive symptoms but not with hyperactive symptoms. Similarly Mazaheri et al. (2013) showed less alpha ERD in inattentive type ADHD patients than in TD controls, but not in combined type ADHD. Gomarus et al. (2009), using a verbal WM task, reported no differences in alpha ERD in a combined-type sample. Diamond (2005) has argued that WM deficits are characteristic of inattentive type ADHD, thus explaining the inconsistent effects of stimulants in this sample. In complementary work, Kuntsi et al. (2001) found that hyperactive children did not differ in WM performance, when controlling for IQ. It is therefore possible that the encoding alpha-ERD related mechanisms are impaired in only a subpopulation of ADHD, defined by inattentive symptoms. Our sample was also unique relative to prior findings in that no differences were present in performance on the SWM task, a further qualification of the sample characteristics.

We also emphasize that the group findings that we report beg replication given the modest sample size of our study. We remain cautiously optimistic as effect sizes were moderate to large for group differences in alpha ERD (EEG, Cohen's $d = .7$; EEG-fMRI, Cohen's $d = .79$) as well as for its neural correlates in occipital activity (Cohen's $d = .88$) and fronto-parieto-occipital connectivity (Cohen's $d = 1.39/2.51$). While effect sizes can be inflated in small-sample studies (Bradley et al., 2002; Button et al., 2013; Yarkoni, 2009), those presented here are consistent with the group effect size that we reported previously for alpha ERD during encoding in a sample of 71 participants (Cohen's $d = .81$). Furthermore, the strength of the interaction between occipital cortex and fronto-parietal cortex with alpha ERD also predicted inattention symptoms ($r(18) = -.6$, $p < .005$). Thus, while a replication is warranted, the combined results suggest that further study of alpha ERD and both occipital activity and network connectivity may inform the mechanisms of ADHD inattention symptoms.

4.3. Concurrent EEG-fMRI recordings in ADHD

Our findings add to a growing literature that demonstrates both the value and difficulty of performing concurrent EEG-fMRI experiments in children (Moeller et al., 2013). However they also caution that excessive motion will contaminate the EEG data, and if not eliminated may

contribute noise, and may bias group contrasts. Elimination of poor quality EEG data can result in high attrition rate (here 9/30; also see Baumeister et al., 2014 for an adult study with 6/23 excluded due to insufficient EEG data quality and technical difficulties). The problem with motion is well appreciated in the literature, most notably in pediatric epilepsy research (Moeller et al., 2013), with some experimenters suggesting sedation to minimize motion (Jacobs et al., 2007; Moeller et al., 2008; Siniatchkin et al., 2007, 2010). This is of course undesirable in task-based experiments. Moosmann et al. (2009) proposed an algorithm that used fMRI-based motion regressors to identify and exclude motion-polluted time intervals from the window-based gradient-artifact cleaning algorithm. In our experience, we found that this approach is appropriate in cases where motion is sporadic and infrequent, but becomes biased and inconsistent if the motion occurs more frequently or in clustered bursts. Another approach (Masterton et al., 2007) places wire coils on the EEG net to measure motion forces on the cap, for subsequent removal. This method also is of limited benefit when motion exceeds 1–2 mm, as can be typical for child participants. An optimal solution for post-hoc motion removal does not yet exist. The emergence of multi-band radiofrequency pulse sequences in fMRI (Feinberg et al., 2010; Moeller et al., 2010) may offer some benefit to concurrent experiments, as these afford faster sampling and thus allow for greater temporal precision in isolating and removing motion artifacts from the data. It may be prudent to eliminate corrupted data until a more rigorous solution is available. We additionally make an effort here to explicitly characterize motion in both excluded and included participants with aim to make the assessment of motion effects on signals of interest transparent and to facilitate comparisons in future studies.

The correlation of motion with between-subject variability, such as ADHD subtype, has implications similar to those already reported with respect to connectivity analyses (Power et al., 2012), for instance, with potential to artificially increase local connectivity and decrease long-range connectivity producing spurious group differences when groups differ in motion (e.g., particularly relevant to comparisons of combined type versus inattentive ADHD participants). Here we implemented a two-step motion correction approach (including motion realignment and ICA denoising), robust regression statistics, and validation group analyses of the motion parameters to minimize motion effects. Nonetheless, a group-related degradation of EEG data remained, indicating robustness of the artifact. It is of note that inclusion of this subgroup in the analyses could inflate the variance in the ADHD sample and lead to bias in detection of group differences, driven by noise not signal. Such dangers necessitate careful attention to removal of motion artifacts or motion-contaminated time points from both fMRI and EEG data, co-varying of motion estimates across subjects in statistical assessments, and/or elimination of subjects from final analysis. Alternatively, the correlation between participant characteristics (e.g., higher hyperactivity symptoms) and motion-induced artifacts argues that EEG-BOLD associations in such patients may be better evaluated using a technique more robust to motion than EEG-fMRI — such as functional near infrared spectroscopy.

5. Conclusion

Using a concurrent EEG-fMRI protocol, we demonstrate that alpha ERD predicts increases in fronto-parieto-occipital connectivity, thus adding to prior reports of association between alpha ERD and occipital activation — which we also observe. We show for the first time that occipital activations were weaker in participants with primarily inattentive type ADHD, whereas fronto-parieto-occipital connectivity was stronger, a finding consistent with a compensatory response of the attentional system in modulating activity within occipital cortex. The results point to a unique, encoding-related, ADHD deficit in fronto-parieto-occipital connectivity that may underlie SWM deficits in at least some individuals with ADHD. Finally, the characteristics of participants excluded from analysis in our study (elevated hyperactivity symptoms and motion parameters), argue that degradation of EEG data by motion-related fMRI artifacts will bias the sample characteristics, a finding with significant implications for experimental design in the clinical setting where such populations are common.

Acknowledgments

This study was supported by a 2012 Fellowship (awarded to A.L.) from The Klingenstein Third Generation Foundation. We acknowledge the Staglin IMHRO Center for Cognitive Neuroscience for its support of the study, as well as Mariem Hussien and Danni Ji for the assistance with data collection.

References

Alderson, R.M., Kasper, L.J., Hudec, K.L., Patros, C.H., 2013. Attention-deficit/hyperactivity disorder (ADHD) and working memory in adults: a meta-analytic review. Neuropsychology 27 (3), 287–302. http://dx.doi.org/10.1037/a0032371.

Allen, P.J., Polizzi, G., Krakow, K., Fish, D.R., Lemieux, L., 1998. Identification of EEG events in the MR scanner: the problem of pulse artifact and a method for its subtraction. NeuroImage 8 (3), 229–239. http://dx.doi.org/10.1006/nimg.1998.0361.

Arnsten, A.F., Rubia, K., 2012. Neurobiological circuits regulating attention, cognitive control, motivation, and emotion: disruptions in neurodevelopmental psychiatric disorders. J. Am. Acad. Child Adolesc. Psychiatry 51 (4), 356–367. http://dx.doi.org/10.1016/j.jaac.2012.01.008.

Awh, E., Jonides, J., 2001. Overlapping mechanisms of attention and spatial working memory. Trends Cogn. Sci. 5 (3), 119–126.

Baddeley, A., 1986. Working Memory. Oxford University Press, New York.

Baddeley, A., 2002. Is working memory still working? Eur. Psychol. 7 (2), 85–97.

Baumeister, S., Hohmann, S., Wolf, I., Plichta, M.M., Rechtsteiner, S., Zangl, M., ... Brandeis, D., 2014. Sequential inhibitory control processes assessed through simultaneous EEG-fMRI. NeuroImage 94, 349–359. http://dx.doi.org/10.1016/j.neuroimage.2014.01.023.

Beckmann, C.F., Smith, S.A., 2004. Probabilistic independent component analysis for functional magnetic resonance imaging. IEEE Trans. Med. Imaging 23 (2), 137–152. http://dx.doi.org/10.1109/Tmi.2003.822821.

Beckmann, C.F., Jenkinson, M., Smith, S.M., 2003. General multilevel linear modeling for group analysis in FMRI. NeuroImage 20 (2), 1052–1063. http://dx.doi.org/10.1016/S1053-8119(03)00435-X.

Bedard, A.C., Newcorn, J.H., Clerkin, S.M., Krone, B., Fan, J., Halperin, J.M., Schulz, K.P., 2014. Reduced prefrontal efficiency for visuospatial working memory in attention-deficit/hyperactivity disorder. J. Am. Acad. Child Adolesc. Psychiatry 53 (9), 1020–1030, e1026. http://dx.doi.org/10.1016/j.jaac.2014.05.011.

Berger, H., 1930. Electroencephalogram of humans. J. Psychol. Neurol. 40, 160–179.

Boecker, R., Holz, N.E., Buchmann, A.F., Blomeyer, D., Plichta, M.M., Wolf, I., ... Laucht, M., 2014. Impact of early life adversity on reward processing in young adults: EEG-fMRI results from a prospective study over 25 years. PLoS One 9 (8), e104185. http://dx.doi.org/10.1371/journal.pone.0104185.

Bollimunta, A., Chen, Y., Schroeder, C.E., Ding, M., 2008. Neuronal mechanisms of cortical alpha oscillations in awake-behaving macaques. J. Neurosci 28 (40), 9976–9988. http://dx.doi.org/10.1523/JNEUROSCI.2699-08.2008.

Bollimunta, A., Mo, J., Schroeder, C.E., Ding, M., 2011. Neuronal mechanisms and attentional modulation of corticothalamic alpha oscillations. J. Neurosci 31 (13), 4935–4943. http://dx.doi.org/10.1523/JNEUROSCI.5580-10.2011.

Boonstra, A.M., Oosterlaan, J., Sergeant, J.A., Buitelaar, J.K., 2005. Executive functioning in adult ADHD: a meta-analytic review. Psychol. Med. 35 (8), 1097–1108. http://dx.doi.org/10.1017/S003329170500499x.

Bradley, M.T., Smith, D., Stoica, G., 2002. A Monte-Carlo estimation of effect size distortion due to significance testing. Percept. Mot. Skills 95 (3 Pt 1), 837–842. http://dx.doi.org/10.2466/pms.2002.95.3.837.

Brainard, D.H., 1997. The psychophysics toolbox. Spat. Vis. 10 (4), 433–436.

Busch, N.A., Dubois, J., VanRullen, R., 2009. The phase of ongoing EEG oscillations predicts visual perception. J. Neurosci 29 (24), 7869–7876. http://dx.doi.org/10.1523/JNEUROSCI.0113-09.2009.

Bush, G., 2010. Attention-deficit/hyperactivity disorder and attention networks. Neuropsychopharmacol. 35 (1), 278–300. http://dx.doi.org/10.1038/npp.2009.120 (npp2009120 [pii]).

Button, K.S., Ioannidis, J.P., Mokrysz, C., Nosek, B.A., Flint, J., Robinson, E.S., Munafo, M.R., 2013. Power failure: why small sample size undermines the reliability of neuroscience. Nat. Rev. Neurosci. 14 (5), 365–376. http://dx.doi.org/10.1038/nrn3475.

Castellanos, F.X., Tannock, R., 2002. Neuroscience of attention-deficit/hyperactivity disorder: the search for endophenotypes. Nat. Rev. Neurosci. 3 (8), 617–628. http://dx.doi.org/10.1038/Nrn896.

Chaumon, M., Busch, N.A., 2014. Prestimulus neural oscillations inhibit visual perception via modulation of response gain. J. Cogn. Neurosci. 26 (11), 2514–2529. http://dx.doi.org/10.1162/jocn_a_00653.

Constantinidis, C., Franowicz, M.N., Goldman-Rakic, P.S., 2001. Coding specificity in cortical microcircuits: a multiple-electrode analysis of primate prefrontal cortex. J. Neurosci 21 (10), 3646–3655.

Cortese, S., Kelly, C., Chabernaud, C., Proal, E., Di Martino, A., Milham, M.P., Castellanos, F.X., 2012. Toward systems neuroscience of ADHD: a meta-analysis of 55 fMRI

studies. Am. J. Psychiatry 169 (10), 1038–1055. http://dx.doi.org/10.1176/appi.ajp.2012.11101521.
de Munck, J.C., Goncalves, S.I., Huijboom, L., Kuijer, J.P., Pouwels, P.J., Heethaar, R.M., Lopes da Silva, F.H., 2007. The hemodynamic response of the alpha rhythm: an EEG/fMRI study. NeuroImage 35 (3), 1142–1151. http://dx.doi.org/10.1016/j.neuroimage.2007.01.022.
Debener, S., Mullinger, K.J., Niazy, R.K., Bowtell, R.W., 2008. Properties of the ballistocardiogram artefact as revealed by EEG recordings at 1.5, 3 and 7 T static magnetic field strength. Int. J. Psychophysiol. 67 (3), 189–199. http://dx.doi.org/10.1016/j.ijpsycho.2007.05.015.
Delorme, A., Makeig, S., 2004. EEGLAB: an open source toolbox for analysis of single-trial EEG dynamics including independent component analysis. J. Neurosci. Methods 134 (1), 9–21. http://dx.doi.org/10.1016/J.Jneumeth.2003.10.009.
Diamond, A., 2005. Attention-deficit disorder (attention-deficit/hyperactivity disorder without hyperactivity): a neurobiologically and behaviorally distinct disorder from attention-deficit/hyperactivity disorder (with hyperactivity). Dev. Psychopathol. 17 (3), 807–825. http://dx.doi.org/10.1017/S0954579405050388.
Doesburg, S.M., Green, J.J., McDonald, J.J., Ward, L.M., 2009. From local inhibition to long-range integration: a functional dissociation of alpha-band synchronization across cortical scales in visuospatial attention. Brain Res. 1303, 97–110. http://dx.doi.org/10.1016/j.brainres.2009.09.069.
Ergenoglu, T., Demiralp, T., Bayraktaroglu, Z., Ergen, M., Beydagi, H., Uresin, Y., 2004. Alpha rhythm of the EEG modulates visual detection performance in humans. Brain Res. Cogn. Brain Res. 20 (3), 376–383. http://dx.doi.org/10.1016/j.cogbrainres.2004.03.009.
Feinberg, D.A., Moeller, S., Smith, S.M., Auerbach, E., Ramanna, S., Gunther, M., ... Yacoub, E., 2010. Multiplexed echo planar imaging for sub-second whole brain FMRI and fast diffusion imaging. PLoS One 5 (12), e15710. http://dx.doi.org/10.1371/journal.pone.0015710.
Foxe, J.J., Snyder, A.C., 2011. The role of alpha-band brain oscillations as a sensory suppression mechanism during selective attention. Front. Psychol. 2, 154. http://dx.doi.org/10.3389/fpsyg.2011.00154.
Freunberger, R., Klimesch, W., Griesmayr, B., Sauseng, P., Gruber, W., 2008. Alpha phase coupling reflects object recognition. NeuroImage 42 (2), 928–935. http://dx.doi.org/10.1016/j.neuroimage.2008.05.020.
Friedman-Hill, S.R., Wagman, M.R., Gex, S.E., Pine, D.S., Leibenluft, E., Ungerleider, L.G., 2010. What does distractibility in ADHD reveal about mechanisms for top-down attentional control? Cognition 115 (1), 93–103. http://dx.doi.org/10.1016/J.Cognition.2009.11.013.
Friston, K.J., Buechel, C., Fink, G.R., Morris, J., Rolls, E., Dolan, R.J., 1997. Psychophysiological and modulatory interactions in neuroimaging. NeuroImage 6 (3), 218–229.
Gitelman, D.R., Penny, W.D., Ashburner, J., Friston, K.J., 2003. Modeling regional and psychophysiologic interactions in fMRI: the importance of hemodynamic deconvolution. NeuroImage 19 (1), 200–207.
Glahn, D.C., Kim, J., Cohen, M.S., Poutanen, V.P., Therman, S., Bava, S., ... Cannon, T.D., 2002. Maintenance and manipulation in spatial working memory: dissociations in the prefrontal cortex. NeuroImage 17 (1), 201–213. http://dx.doi.org/10.1006/Nimg.2002.1161.
Glover, G.H., 1999. Deconvolution of impulse response in event-related BOLD fMRI. NeuroImage 9 (4), 416–429.
Goldman, R.I., Stern, J., Engel, J., Cohen, M., 2001. Tomographic mapping of alpha rhythm using simultaneous EEG/fMRI. NeuroImage 13 (6), S1291.
Goldman, R.I., Stern, J.M., Engel Jr., J., Cohen, M.S., 2002. Simultaneous EEG and fMRI of the alpha rhythm. Neuroreport 13 (18), 2487–2492. http://dx.doi.org/10.1097/01.wnr.0000047685.08940.d0.
Gomarus, H.K., Wijers, A.A., Minderaa, R.B., Althaus, M., 2009. Do children with ADHD and/or PDD-NOS differ in reactivity of alpha/theta ERD/ERS to manipulations of cognitive load and stimulus relevance? Clin. Neurophysiol. 120 (1), 73–79. http://dx.doi.org/10.1016/j.clinph.2008.10.017.
Goncalves, S.I., de Munck, J.C., Pouwels, P.J., Schoonhoven, R., Kuijer, J.P., Maurits, N.M., ... Lopes da Silva, F.H., 2006. Correlating the alpha rhythm to BOLD using simultaneous EEG/fMRI: inter-subject variability. NeuroImage 30 (1), 203–213. http://dx.doi.org/10.1016/j.neuroimage.2005.09.062.
Hanslmayr, S., Klimesch, W., Sauseng, P., Gruber, W., Doppelmayr, M., Freunberger, R., Pecherstorfer, T., 2005. Visual discrimination performance is related to decreased alpha amplitude but increased phase locking. Neurosci. Lett. 375 (1), 64–68. http://dx.doi.org/10.1016/j.neulet.2004.10.092.
Hanslmayr, S., Aslan, A., Staudigl, T., Klimesch, W., Herrmann, C.S., Bauml, K.H., 2007. Prestimulus oscillations predict visual perception performance between and within subjects. NeuroImage 37 (4), 1465–1473. http://dx.doi.org/10.1016/j.neuroimage.2007.07.011.
Hauser, T.U., Iannaccone, R., Ball, J., Mathys, C., Brandeis, D., Walitza, S., Brem, S., 2014. Role of the medial prefrontal cortex in impaired decision making in juvenile attention-deficit/hyperactivity disorder. JAMA Psychiatry 71 (10), 1165–1173. http://dx.doi.org/10.1001/jamapsychiatry.2014.1093.
Huang-Pollock, C.L., Nigg, J.T., 2003. Searching for the attention deficit in attention deficit hyperactivity disorder: the case of visuospatial orienting. Clin. Psychol. Rev. 23 (6), 801–830. http://dx.doi.org/10.1016/S0272-7358(03)00073-4.
Huang-Pollock, C.L., Carr, T.H., Nigg, J.T., 2002. Development of selective attention: perceptual load influences early versus late attentional selection in children and adults. Dev. Psychol. 38 (3), 363–375. http://dx.doi.org/10.1037//0012-1649.38.3.363.
Huang-Pollock, C.L., Nigg, J.T., Carr, T.H., 2005. Deficient attention is hard to find: applying the perceptual load model of selective attention to attention deficit hyperactivity disorder subtypes. J. Child Psychol. Psychiatry 46 (11), 1211–1218. http://dx.doi.org/10.1111/J.1469–7610.2005.00410.X.
Huang-Pollock, C.L., Nigg, J.T., Halperin, J.M., 2006. Single dissociation findings of ADHD deficits in vigilance but not anterior or posterior attention systems. Neuropsychology 20 (4), 420–429. http://dx.doi.org/10.1037/0894–4105.20.4.420.
Huang-Pollock, C.L., Karalunas, S.L., Tam, H., Moore, A.N., 2012. Evaluating vigilance deficits in ADHD: a meta-analysis of CPT performance. J. Abnorm. Psychol. 121 (2), 360–371. http://dx.doi.org/10.1037/a0027205.
Hummel, F., Gerloff, C., 2005. Larger interregional synchrony is associated with greater behavioral success in a complex sensory integration task in humans. Cereb. Cortex 15 (5), 670–678. http://dx.doi.org/10.1093/cercor/bhh170.
Jacobs, J., Kobayashi, E., Boor, R., Muhle, H., Stephan, W., Hawco, C., ... Siniatchkin, M., 2007. Hemodynamic responses to interictal epileptiform discharges in children with symptomatic epilepsy. Epilepsia 48 (11), 2068–2078. http://dx.doi.org/10.1111/j.1528-1167.2007.01192.x.
Jensen, O., Gelfand, J., Kounios, J., Lisman, J.E., 2002. Oscillations in the alpha band (9–12 Hz) increase with memory load during retention in a short-term memory task. Cereb. Cortex 12 (8), 877–882.
Karch, S., Thalmeier, T., Lutz, J., Cerovecki, A., Opgen-Rhein, M., Hock, B., ... Pogarell, O., 2010. Neural correlates (ERP/fMRI) of voluntary selection in adult ADHD patients. Eur. Arch. Psychiatry Clin. Neurosci. 260 (5), 427–440. http://dx.doi.org/10.1007/s00406-009-0089-y.
Karch, S., Voelker, J.M., Thalmeier, T., Ertl, M., Leicht, G., Pogarell, O., Mulert, C., 2014. Deficits during voluntary selection in adult patients with ADHD: new insights from single-trial coupling of simultaneous EEG/fMRI. Front. Psychol. 5, 41. http://dx.doi.org/10.3389/fpsyt.2014.00041.
Kaufman, J., Birmaher, B., Brent, D., Rao, U., Flynn, C., Moreci, P., ... Ryan, N., 1997. Schedule for affective disorders and schizophrenia for school-age children present and lifetime version (K-SADS-PL): initial reliability and validity data. J. Am. Acad. Child Adolesc. Psychiatry 36 (7), 980–988.
Kirschfeld, K., 2005. The physical basis of alpha waves in the electroencephalogram and the origin of the "Berger effect". Biol. Cybern. 92 (3), 177–185. http://dx.doi.org/10.1007/s00422-005-0547-1.
Kleiner, M., Brainard, D., Pelli, D., 2007. What's new in psychtoolbox-3? Perception 36, 14-14.
Klimesch, W., 1997. EEG-alpha rhythms and memory processes. Int. J. Psychophysiol. 26 (1–3), 319–340.
Klimesch, W., 1999. EEG alpha and theta oscillations reflect cognitive and memory performance: a review and analysis. Brain Res. Rev. 29 (2–3), 169–195.
Klimesch, W., 2012. Alpha-band oscillations, attention, and controlled access to stored information. Trends Cogn. Sci. 16 (12), 606–617. http://dx.doi.org/10.1016/j.tics.2012.10.007.
Klimesch, W., Doppelmayr, M., Schimke, H., Ripper, B., 1997. Theta synchronization and alpha desynchronization in a memory task. Psychophysiology 34 (2), 169–176.
Klimesch, W., Sauseng, P., Hanslmayr, S., 2007. EEG alpha oscillations: the inhibition-timing hypothesis. Brain Res. Rev. 53 (1), 63–88. http://dx.doi.org/10.1016/J.Brainresrev.2006.06.003.
Klimesch, W., Fellinger, R., Freunberger, R., 2011. Alpha oscillations and early stages of visual encoding. Front. Psychol. 2, 118. http://dx.doi.org/10.3389/fpsyg.2011.00118.
Kofler, M.J., Rapport, M.D., Sarver, D.E., Raiker, J.S., Orban, S.A., Friedman, L.M., Kolomeyer, E.G., 2013. Reaction time variability in ADHD: a meta-analytic review of 319 studies. Clin. Psychol. Rev. 33 (6), 795–811. http://dx.doi.org/10.1016/j.cpr.2013.06.001.
Kuntsi, J., Oosterlaan, J., Stevenson, J., 2001. Psychological mechanisms in hyperactivity: I. response inhibition deficit, working memory impairment, delay aversion, or something else? J. Child Psychol Psychiatry 42 (2), 199–210.
Lange, J., Oostenveld, R., Fries, P., 2013. Reduced occipital alpha power indexes enhanced excitability rather than improved visual perception. J. Neurosci 33 (7), 3212–3220. http://dx.doi.org/10.1523/JNEUROSCI.3755-12.2013.
Laufs, H., Kleinschmidt, A., Beyerle, A., Eger, E., Salek-Haddadi, A., Preibisch, C., Krakow, K., 2003. EEG-correlated fMRI of human alpha activity. NeuroImage 19 (4), 1463–1476. http://dx.doi.org/10.1016/S1053-8119(03)00286-6.
Lee, T.W., Girolami, M., Sejnowski, T.J., 1999. Independent component analysis using an extended infomax algorithm for mixed subgaussian and supergaussian sources. Neural Comput. 11 (2), 417–441.
Lenartowicz, A., Delorme, A., Walshaw, P.D., Cho, A.L., Bilder, R.M., McGough, J.J., ... Loo, S.K., 2014. Electroencephalography correlates of spatial working memory deficits in attention-deficit/hyperactivity disorder: vigilance, encoding, and maintenance. J. Neurosci 34 (4), 1171–1182. http://dx.doi.org/10.1523/JNEUROSCI.1765-13.2014.
Liu, Y., Bengson, J., Huang, H., Mangun, G.R., Ding, M., 2014. Top-down modulation of neural activity in anticipatory visual attention: control mechanisms revealed by simultaneous EEG-fMRI. Cereb. Cortex http://dx.doi.org/10.1093/cercor/bhu204.
Loo, S.K., Humphrey, L.A., Tapio, T., Moilanen, I.K., McGough, J.J., McCracken, J.T., ... Smalley, S.L., 2007. Executive functioning among Finnish adolescents with attention-deficit/hyperactivity disorder. J. Am. Acad. Child Adolesc. Psychiatry 46 (12), 1594–1604. http://dx.doi.org/10.1097/chi.0b013e3181575014.
Lopes da Silva, F.H., 1991. Neural mechanisms underlying brain waves: from neural membranes to networks. Electroencephalogr Clin. Neurophysiol. 79 (2), 81–93.
Lopes da Silva, F.H., Vos, J.E., Mooibroek, J., Van Rotterdam, A., 1980. Relative contributions of intracortical and thalamo-cortical processes in the generation of alpha rhythms, revealed by partial coherence analysis. Electroencephalogr Clin. Neurophysiol. 50 (5–6), 449–456.
Luchinger, R., Michels, L., Martin, E., Brandeis, D., 2011. EEG-BOLD correlations during (post-)adolescent brain maturation. NeuroImage 56 (3), 1493–1505. http://dx.doi.org/10.1016/j.neuroimage.2011.02.050.
Luchinger, R., Michels, L., Martin, E., Brandeis, D., 2012. Brain state regulation during normal development: intrinsic activity fluctuations in simultaneous EEG-fMRI. NeuroImage 60 (2), 1426–1439. http://dx.doi.org/10.1016/j.neuroimage.2012.01.031.
Martinussen, R., Hayden, J., Hogg-Johnson, S., Tannock, R., 2005. A meta-analysis of working memory impairments in children with attention-deficit/hyperactivity disorder. J. Am. Acad. Child Adolesc. Psychiatry 44 (4), 377–384. http://dx.doi.org/10.1097/01.Chi.0000153228.72591.73.

Mason, D.J., Humphreys, G.W., Kent, L.S., 2003. Exploring selective attention in ADHD: visual search through space and time. J. Child Psychol. Psychiatry 44 (8), 1158–1176.
Mason, D.J., Humphreys, G.W., Kent, L., 2005. Insights into the control of attentional set in ADHD using the attentional blink paradigm. J. Child Psychol. Psychiatry 46 (12), 1345–1353. http://dx.doi.org/10.1111/j.1469-7610.2005.01428.x.
Masterton, R.A., Abbott, D.F., Fleming, S.W., Jackson, G.D., 2007. Measurement and reduction of motion and ballistocardiogram artefacts from simultaneous EEG and fMRI recordings. NeuroImage 37 (1), 202–211. http://dx.doi.org/10.1016/j.neuroimage.2007.02.060.
Mathewson, K.E., Lleras, A., Beck, D.M., Fabiani, M., Ro, T., Gratton, G., 2011. Pulsed out of awareness: EEG alpha oscillations represent a pulsed-inhibition of ongoing cortical processing. Front. Psychol. 2, 99. http://dx.doi.org/10.3389/fpsyg.2011.00099.
Mazaheri, A., Coffey-Corina, S., Mangun, G.R., Bekker, E.M., Berry, A.S., Corbett, B.A., 2010. Functional disconnection of frontal cortex and visual cortex in attention-deficit/hyperactivity disorder. Biol. Psychiatry 67 (7), 617–623. http://dx.doi.org/10.1016/J.Biopsych.2009.11.022.
Mazaheri, A., Fassbender, C., Coffey-Corina, S., Hartanto, T.A., Schweitzer, J.B., Mangun, G.R., 2013. Differential oscillatory electroencephalogram between attention-deficit/hyperactivity disorder subtypes and typically developing adolescents. Biol. Psychiatry http://dx.doi.org/10.1016/j.biopsych.2013.08.023.
McLaren, D.G., Ries, M.L., Xu, G., Johnson, S.C., 2012. A generalized form of context-dependent psychophysiological interactions (gPPI): a comparison to standard approaches. NeuroImage 61 (4), 1277–1286. http://dx.doi.org/10.1016/j.neuroimage.2012.03.068.
Meltzer, J.A., Negishi, M., Mayes, L.C., Constable, R.T., 2007. Individual differences in EEG theta and alpha dynamics during working memory correlate with fMRI responses across subjects. Clin. Neurophysiol. 118 (11), 2419–2436. http://dx.doi.org/10.1016/j.clinph.2007.07.023.
Michels, L., Bucher, K., Luchinger, R., Klaver, P., Martin, E., Jeanmonod, D., Brandeis, D., 2010. Simultaneous EEG-fMRI during a working memory task: modulations in low and high frequency bands. PLoS One 5 (4), e10298. http://dx.doi.org/10.1371/journal.pone.0010298.
Michels, L., Luchinger, R., Koenig, T., Martin, E., Brandeis, D., 2012. Developmental changes of BOLD signal correlations with global human EEG power and synchronization during working memory. PLoS One 7 (7), e39447. http://dx.doi.org/10.1371/journal.pone.0039447.
Missonnier, P., Hasler, R., Perroud, N., Herrmann, F.R., Millet, P., Richiardi, J., ... Baud, P., 2013. EEG anomalies in adult ADHD subjects performing a working memory task. Neuroscience 241, 135–146. http://dx.doi.org/10.1016/j.neuroscience.2013.03.011.
Mo, J., Schroeder, C.E., Ding, M., 2011. Attentional modulation of alpha oscillations in macaque inferotemporal cortex. J. Neurosci. 31 (3), 878–882. http://dx.doi.org/10.1523/JNEUROSCI.5295-10.2011.
Moeller, F., Siebner, H.R., Wolff, S., Muhle, H., Boor, R., Granert, O., ... Siniatchkin, M., 2008. Changes in activity of striato–thalamo–cortical network precede generalized spike wave discharges. NeuroImage 39 (4), 1839–1849. http://dx.doi.org/10.1016/j.neuroimage.2007.10.058.
Moeller, S., Yacoub, E., Olman, C.A., Auerbach, E., Strupp, J., Harel, N., Ugurbil, K., 2010. Multiband multislice GE-EPI at 7 tesla, with 16-fold acceleration using partial parallel imaging with application to high spatial and temporal whole-brain fMRI. Magn. Reson. Med. 63 (5), 1144–1153. http://dx.doi.org/10.1002/mrm.22361.
Moeller, F., Stephani, U., Siniatchkin, M., 2013. Simultaneous EEG and fMRI recordings (EEG-fMRI) in children with epilepsy. Epilepsia 54 (6), 971–982. http://dx.doi.org/10.1111/epi.12197.
Moosmann, M., Ritter, P., Krastel, I., Brink, A., Thees, S., Blankenburg, F., ... Villringer, A., 2003. Correlates of alpha rhythm in functional magnetic resonance imaging and near infrared spectroscopy. NeuroImage 20 (1), 145–158.
Moosmann, M., Schonfelder, V.H., Specht, K., Scheeringa, R., Nordby, H., Hugdahl, K., 2009. Realignment parameter-informed artefact correction for simultaneous EEG-fMRI recordings. NeuroImage 45 (4), 1144–1150. http://dx.doi.org/10.1016/j.neuroimage.2009.01.024.
Mullinger, K.J., Havenhand, J., Bowtell, R., 2013. Identifying the sources of the pulse artefact in EEG recordings made inside an MR scanner. NeuroImage 71, 75–83. http://dx.doi.org/10.1016/j.neuroimage.2012.12.070.
Nigg, J.T., 2005. Neuropsychologic theory and findings in attention-deficit/hyperactivity disorder: the state of the field and salient challenges for the coming decade. Biol. Psychiatry 57 (11), 1424–1435. http://dx.doi.org/10.1016/j.biopsych.2004.11.011.
Nigg, J.T., Swanson, J.M., Hinshaw, S.P., 1997. Covert visual spatial attention in boys with attention deficit hyperactivity disorder: lateral effects, methylphenidate response and results for parents. Neuropsychologia 35 (2), 165–176.
Oberlin, B.G., Alford, J.L., Marrocco, R.T., 2005. Normal attention orienting but abnormal stimulus alerting and conflict effect in combined subtype of ADHD. Behav. Brain Res. 165 (1), 1–11. http://dx.doi.org/10.1016/J.Bbr.2005.06.041.
Palva, S., Palva, J.M., 2007. New vistas for alpha-frequency band oscillations. Trends Neurosci. 30 (4), 150–158. http://dx.doi.org/10.1016/j.tins.2007.02.001.
Palva, S., Palva, J.M., 2011. Functional roles of alpha-band phase synchronization in local and large-scale cortical networks. Front. Psychol. 2, 204. http://dx.doi.org/10.3389/fpsyg.2011.00204.
Power, J.D., Barnes, K.A., Snyder, A.Z., Schlaggar, B.L., Petersen, S.E., 2012. Spurious but systematic correlations in functional connectivity MRI networks arise from subject motion. NeuroImage 59 (3), 2142–2154. http://dx.doi.org/10.1016/j.neuroimage.2011.10.018.
Rihs, T.A., Michel, C.M., Thut, G., 2007. Mechanisms of selective inhibition in visual spatial attention are indexed by alpha-band EEG synchronization. Eur. J. Neurosci. 25 (2), 603–610. http://dx.doi.org/10.1111/j.1460-9568.2007.05278.x.
Rodriguez, C.D., Lenartowicz, A., Cohen, M.S., 2013. An EKG-free Method for Extracting BCG Timing From the EEG Signal. Paper presented at the International Conference on Basic and Clinical Mulitmodal Imaging, Geneva.
Romei, V., Brodbeck, V., Michel, C., Amedi, A., Pascual-Leone, A., Thut, G., 2008. Spontaneous fluctuations in posterior alpha-band EEG activity reflect variability in excitability of human visual areas. Cereb. Cortex 18 (9), 2010–2018. http://dx.doi.org/10.1093/Cercor/Bhm229.
Romei, V., Gross, J., Thut, G., 2010. On the role of prestimulus alpha rhythms over occipito-parietal areas in visual input regulation: correlation or causation? J. Neurosci 30 (25), 8692–8697. http://dx.doi.org/10.1523/JNEUROSCI.0160-10.2010.
Rubia, K., Alegria, A.A., Cubillo, A.I., Smith, A.B., Brammer, M.J., Radua, J., 2013. Effects of stimulants on brain function in attention-deficit/hyperactivity disorder: a systematic review and meta-analysis. Biol. Psychiatry http://dx.doi.org/10.1016/j.biopsych.2013.10.016.
Rubia, K., Alegria, A., Brinson, H., 2014. Imaging the ADHD brain: disorder-specificity, medication effects and clinical translation. Expert. Rev. Neurother. 14 (5), 519–538. http://dx.doi.org/10.1586/14737175.2014.907526.
Salimi-Khorshidi, G., Douaud, G., Beckmann, C.F., Glasser, M.F., Griffanti, L., Smith, S.M., 2014. Automatic denoising of functional MRI data: combining independent component analysis and hierarchical fusion of classifiers. NeuroImage 90, 449–468. http://dx.doi.org/10.1016/j.neuroimage.2013.11.046.
Sauseng, P., Klimesch, W., Doppelmayr, M., Pecherstorfer, T., Freunberger, R., Hanslmayr, S., 2005. EEG alpha synchronization and functional coupling during top-down processing in a working memory task. Hum. Brain Mapp. 26 (2), 148–155. http://dx.doi.org/10.1002/Hbm.20150.
Scheeringa, R., Petersson, K.M., Oostenveld, R., Norris, D.G., Hagoort, P., Bastiaansen, M.C., 2009. Trial-by-trial coupling between EEG and BOLD identifies networks related to alpha and theta EEG power increases during working memory maintenance. NeuroImage 44 (3), 1224–1238. http://dx.doi.org/10.1016/j.neuroimage.2008.08.041.
Scheeringa, R., Petersson, K.M., Kleinschmidt, A., Jensen, O., Bastiaansen, M.C., 2012. EEG alpha power modulation of fMRI resting-state connectivity. Brain Connect. 2 (5), 254–264. http://dx.doi.org/10.1089/brain.2012.0088.
Sergeant, J.A., 2005. Modeling attention-deficit/hyperactivity disorder: a critical appraisal of the cognitive-energetic model. Biol. Psychiatry 57 (11), 1248–1255. http://dx.doi.org/10.1016/J.Bps.2004.09.010.
Siniatchkin, M., Moeller, F., Jacobs, J., Stephani, U., Boor, R., Wolff, S., ... Scherg, M., 2007. Spatial filters and automated spike detection based on brain topographies improve sensitivity of EEG-fMRI studies in focal epilepsy. NeuroImage 37 (3), 834–843. http://dx.doi.org/10.1016/j.neuroimage.2007.05.049.
Siniatchkin, M., Groening, K., Moehring, J., Moeller, F., Boor, R., Brodbeck, V., ... Stephani, U., 2010. Neuronal networks in children with continuous spikes and waves during slow sleep. Brain 133 (9), 2798–2813. http://dx.doi.org/10.1093/brain/awq183.
Smith, Edward E., Jonides, John, 1997. Working memory: a view from neuroimaging. Cogn. Psychol. 33, 5–42.
Smith, S.M., Jenkinson, M., Woolrich, M.W., Beckmann, C.F., Behrens, T.E.J., Johansen-Berg, H., ... Matthews, P.M., 2004. Advances in functional and structural MR image analysis and implementation as FSL. NeuroImage 23, S208–S219. http://dx.doi.org/10.1016/J.Neuroimage.2004.07.051.
Sternberg, S., 1966. High-speed scanning in human memory. Science 153 (3736), 652–654.
Stevens, A.A., Maron, L., Nigg, J.T., Cheung, D., Ester, E.F., Awh, E., 2012. Increased sensitivity to perceptual interference in adults with attention deficit hyperactivity disorder. J. Int. Neuropsychol. Soc. 18 (3), 511–520. http://dx.doi.org/10.1017/S1355617712000033.
Swanson, J., Schuck, S., Mann, M., Carlson, C., Hartman, K., Sergeant, J., ... McClearly, R., 2006. Categorical and Dimensional Definitions and Evaluations of Symptoms of ADHD: the SNAP and SWAN Rating Scales. University of California, Irvine.
Thut, G., Nietzel, A., Brandt, S.A., Pascual-Leone, A., 2006. Alpha-band electroencephalographic activity over occipital cortex indexes visuospatial attention bias and predicts visual target detection. J. Neurosci 26 (37), 9494–9502. http://dx.doi.org/10.1523/JNEUROSCI.0875-06.2006.
von Stein, A., Chiang, C., Konig, P., 2000. Top-down processing mediated by interareal synchronization. Proc. Natl. Acad. Sci. U. S. A. 97 (26), 14748–14753. http://dx.doi.org/10.1073/pnas.97.26.14748.
Westerberg, H., Hirvikoski, T., Forssberg, H., Klingberg, T., 2004. Visuo-spatial working memory span: a sensitive measure of cognitive deficits in children with ADHD. Child Neuropsychol. 10 (3), 155–161.
Willcutt, E.G., Doyle, A.E., Nigg, J.T., Faraone, S.V., Pennington, B.F., 2005. Validity of the executive function theory of attention-deficit/hyperactivity disorder: a meta-analytic review. Biol. Psychiatry 57 (11), 1336–1346. http://dx.doi.org/10.1016/j.biopsych.2005.02.006.
Wolf, R.C., Plichta, M.M., Sambataro, F., Fallgatter, A.J., Jacob, C., Lesch, K.P., ... Vasic, N., 2009. Regional brain activation changes and abnormal functional connectivity of the ventrolateral prefrontal cortex during working memory processing in adults with attention-deficit/hyperactivity disorder. Hum. Brain Mapp. 30 (7), 2252–2266. http://dx.doi.org/10.1002/hbm.20665.
Woolrich, M., 2008. Robust group analysis using outlier inference. NeuroImage 41 (2), 286–301. http://dx.doi.org/10.1016/J.Neuroimage.2008.02.042.
Woolrich, M., Ripley, B.D., Brady, M., Smith, S.M., 2001. Temporal autocorrelation in univariate linear modeling of FMRI data. NeuroImage 14 (6), 1370–1386.
Worsley, K.J., Friston, K.J., 1995. Analysis of fMRI time-series revisited—again. NeuroImage 2 (3), 173–181. http://dx.doi.org/10.1006/nimg.1995.1023.
Wyart, V., Tallon-Baudry, C., 2009. How ongoing fluctuations in human visual cortex predict perceptual awareness: baseline shift versus decision bias. J. Neurosci 29 (27), 8715–8725. http://dx.doi.org/10.1523/JNEUROSCI.0962-09.2009.
Yarkoni, T., 2009. Big correlations in little studies: inflated fMRI correlations reflect low statistical power—commentary on Vul et al. (2009). Perspect. Psychol. Sci. 4 (3), 294–298. http://dx.doi.org/10.1111/J.1745–6924.2009.01127.X.